Smart Energy 11 (2023) 100114

Contents lists available at ScienceDirect

Smart Energy

journal homepage: www.journals.elsevier.com/smart-energy

Assessment of paper industry decarbonization potential via hydrogen in a multi-energy system scenario: A case study

Alessandro Mati *, Andrea Ademollo, Carlo Carcasci

Università degli Studi di Firenze, Department of Industrial Engineering, Via di Santa Marta 3, 50139, Firenze, Italy

ARTICLE INFO

Keywords:
Green hydrogen
Hydrogen gas turbine cogeneration plant
Power-to-X
Multi-energy systems
Paper mill

ABSTRACT

Green hydrogen is currently regarded as a key catalyst for the decarbonization of energy-intensive industries. In this context, the pulp and paper industry stands out as one of the most demanding, given the simultaneous need for large amounts of heat and electricity usually satisfied via cogeneration systems. Given the urgent need for cost-effective solutions in response to the climate crisis, it is crucial to analyze the feasibility of retrofitting existing power plants to operate carbon-neutral. The aim of this work is to provide a techno-economic analysis for the conversion of a conventional cogeneration system to run on locally produced hydrogen. Building on the energy consumption of the paper mill, the operation of a hydrogen-fuelled gas turbine is modelled in detail. Based on these results, a multi-energy system model for the production of green fuel is presented, considering production via solar-powered PEM electrolyzers, storage in tanks and final use in the gas turbine. An optimal configuration for the system is defined, leading to the definition of a solution that ensures a cost of 6.41 /kg for the production of green hydrogen. Finally, a sensitivity analysis highlights the close dependence of the economic profitability of the Power-to-X system on the natural gas price. The results indicate that although positive performance is achieved, the cost of investment remains still prohibitive for systems of this size, and the high initial capital expenditure needs to be supported by incentive policies that facilitate the adoption of hydrogen in industrial applications making it competitive in the short term.

1. Introduction

Averaged temperatures around the globe have been rapidly increasing in recent years. Human contribution to the global surface temperature rise has been estimated to be 1.09 °C by the intergovernmental panel on climate change above pre-industrial levels [1]. Climate change, resulting from anthropogenic emissions of greenhouse gases, presents a significant challenge to society and the international community has acknowledged the necessity for mitigation and adaptation efforts through the adoption of the Paris Agreement [2], which aims to limit global warming to below 2°C and achieve carbon neutrality. In line with this, the European Union has presented the European Green Deal, a strategy aimed at achieving net-zero greenhouse gas emissions by 2050 [3]. The success of such initiative hinges on tackling the decarbonization of key sectors such as power generation and industry, by progressively ramping up Renewable Energy Sources (RES) consumption by a 32% up to a 100% increase by 2030 and 2050, respectively [4].

According to the IEA [5], in 2021 the industrial sector accounted for about 38% (169 EJ) of the global final energy use, and was responsible for the emission of 9.4 Gt of CO_2 equivalent to a quarter of global emissions (not considering indirect emissions from the electricity employed in industrial processes). In the perspective of meeting the Net Zero Emissions by 2050 targets [6], industrial emissions should decrease to 7 Gt CO_2 by 2030, following trend opposite to the expected growth in industrial production. Although some moderate progress has been already achieved both in terms of energy efficiency, renewable energy deployment and related policies, significant progress still falls far short of desired goals. Faster development and adoption of low-carbon productive processes, including carbon capture and storage and hydrogen, represent key enablers for meeting this challenge.

1.1. Research context

As the global fourth largest industrial energy consumer, the pulp and paper industry made up about 5% of the total industrial final energy consumption and reported 2% of the sector direct CO_2 emissions [7,8]. Globally, demand and production of pulp and paper is expected to increase significantly by 2050, thus driving up the associated absolute

* Corresponding author.
E-mail addresses: alessandro.mati@unifi.it (A. Mati), andrea.ademollo@unifi.it (A. Ademollo), carlo.carcasci@unifi.it (C. Carcasci).

https://doi.org/10.1016/j.segy.2023.100114
Received 7 March 2023; Received in revised form 13 July 2023; Accepted 13 July 2023
Available online 14 July 2023

energy use and greenhouse gas emissions [9].

The need for an improvement in the energy performance of paper mills is a longstanding issue, and dates back to Thompson et al. [10] studies. Bandher et al. [11] developed a model to estimate emissions behavior from a paper mill facility when switching fuel, installing air pollution devices and undertaking energy efficiency actions. Increasing attention has been put in recent years in rationalizing the usage of energy in the field, focusing also on the valorization of waste streams as in the work form Monte et al. [12]. Decarbonization strategies have been investigated through the examination of utilizing renewable biomass or waste from the facility as energy sources, as well as the implementation of carbon capture technologies [13,14]. A feasibility study, described in Ref. [15], has been conducted to evaluate the energy saving potential and economic benefits of various cogeneration options in a paper mill. The systems analyzed include gas turbine, steam turbine, and combined cycle cogeneration options, which were evaluated and compared based on their energy utilization factor and annualized life cycle cost analysis.

Considering multi-energy systems, hydrogen has recently been investigated as a potential alternative for both power generation and storage. Canan et al. [16] have evaluated the environmental impact, production costs, energy efficiency and exergy efficiency of various methods of hydrogen production from renewable and non-renewable sources. Astiaso Garcia et al. [17] conducted a survey and analysis of the potential of hydrogen as energy storage systems in EU countries, to mitigate the fluctuations in energy supply and negative impacts arising from increased integration of renewable energy sources in power generation. Guandalini et al. [18] have investigated the use of Power-to-Gas systems combined with wind farms to enhance the dispatchability.

Briefly outlining the paper production process, it begins with the production of cellulose pulp. Pulp is produced through the separation of lignin and cellulose fibres from wood and constitutes the basic processing material to produce paper. The wet pulp is bleached and further processed before being dried and pressed to be finally turned into sheets of paper. Due to the nature of its processes, the pulp and paper industry is characterised by high electricity and heat consumption, which means it is well suited for the adoption of cogeneration technologies. This opens up the possibility of investigating innovative solutions and process combinations to help decarbonize the sector [19–21]. Since heat is required in the process of drying the mid-products while electricity is contemporarily employed to operate the machines, cogeneration systems have been widely adopted globally as an efficient and cost-effective strategy to meet paper mills energy demand.

Cogeneration is usually referred as Combined Heat and Power (CHP) and indicates the simultaneous production of process heat and electricity from a single energy source. Several types of power systems can be employed (e.g., internal combustion engines, gas turbines, steam turbines, combined cycle power plants); extracted heat varies widely in magnitude and temperature with differing technology, size and operating parameters [22–24]. The inherent characteristic of these systems is the efficiency improvement in fuel utilization: the combined production of heat and electricity is proved to be more efficient compared to the separate production of the two forms of energy.

CHP systems can play a significant role in complying with the latest environmental regulations and as presented by Kong et al. [21] are perfectly placed in the spectrum of energy-efficient technologies to be adopted by the paper industry, showing the perk of improving the global efficiency of the plant. In this perspective, Yamaki et al. [25] investigate the possibility for paper mills to operate as cogeneration energy hubs, in which the various industrial sites are assumed to sell electricity to the grid and heat to the vicinity with additional fuels and wind power, using in-house utility facilities. In this context, Gas Turbine (GT) based CHP systems have a long record in literature and are widely adopted worldwide for this type of applications [26,27]. The waste heat contained in the exhaust gases from the GT is usually recovered through a Heat Recovery Steam Generator (HRSG) [28], with thermal energy possibly constituting up to 70% of the chemical energy of the inlet fuel. Exhaust gases temperature typically fall in a (720÷870) K temperature range, that depends on the specific application, while stack temperature must be kept above 400 K because of the acid dew point limits depending on the type of fuel used.

Generally, gas turbines with a nominal power of less than 50 MW, easily find application in cogeneration layouts due to their good economic performance and the minor system complexity [29]. In the search for better performance a wide range of innovative solutions have been tested such as the exploitation of biomass gasification [15] and also the employment of some of process waste stream like black liquor has been considered [30]. Dodds et al. [31] have analyzed the need for inclusion of hydrogen and fuel cell heating technologies in future scenario analyses, highlighting the significance for policymakers to consider the full potential of hydrogen and fuel cells in low-carbon energy systems. Skordoulias et al. [32] have presented a study that provides insights of a medium-scale GT-based cogeneration system powered via renewable hydrogen production and use. They present Levelized Cost of Hydrogen (LCOH) production values for different natural gas substitution scenarios and variations in the EU Emissions Trading System (ETS) carbon prices as for present and projected trends.

1.2. Green hydrogen in the energy intensive industry

The integration of different sectors (e.g., electricity, heat, traditional fuels, hydrogen and Power-to-X fuels) within the holistic framework of "Smart Energy Systems" (as defined by Lund et al. [33]) is a powerful approach that enables the identification of viable and sustainable solutions through the intelligent management of a complete set of different energy forms. This is especially relevant it the industrial and transport sectors [34,35] where power-to-gas concept offers a framework to explore solutions for integrating fluctuating renewable energy.

In the context of decarbonizing the heavy and energy intensive industries, hydrogen is considered to be one of the most promising carbon-free energy carriers, which can be produced from both fossil and renewable energy sources [36–38]. A comprehensive study by Johannsen et al. [39] analyzed the complete replacement of fossil fuels in the European industrial sector by renewable energy, addressing energy efficiency and fossil fuel substitution measures based on current and innovative technologies. While the primary focus is on energy efficiency and electrification, the utilization of hydrogen in the transition is also considered, with a specific emphasis on high-temperature processes. As for the paper and pulp industry, the use of hydrogen boilers is examined for steam generation.

Green hydrogen, produced by exploiting enewable energy sources surplus, enables the storage of renewable energy which can then be converted back into electricity as needed. Power-to-Gas (PtG) hydrogen is a key area of interest for hydrogen economy roadmaps, given the need to integrate more RES into the energy system [40]. Hydrogen versatility makes it a highly desirable energy carrier, as it can be rapidly converted into mechanical, thermal, and electrical energy through the use of internal combustion engines, steam engines, and fuel cells [41]. Its combustion is also more efficient and cleaner than petrochemicals, resulting in low emissions when used as a fuel source for vehicles [42], representing a suitable fuel also for domestic and industrial heating applications. Recent developments have also highlighted its potential to improve the flexibility of power plants and make them "hydrogen ready" as the demand for renewable energy storage increases and hydrogen infrastructure strengthens.

The feasibility of using green hydrogen with current thermal power plants, specifically gas turbine fleets, is a crucial factor to consider. By retrofitting existing GT combustors and boilers, high-temperature heat can be produced from hydrogen. Hydrogen can therefore replace natural gas in existing power plants with only minor modifications [40]. In recent years, a cooperation agreement was signed between the German energy utility Uniper and Siemens Gas and Power to create projects focused on the decarbonization of power generation and the use of green

hydrogen [43]. One of the most noteworthy examples in this sense is represented by a joint venture of European companies, research institutes, and universities that has launched the world's first demonstration of a completely integrated power-to-hydrogen-to-power project on an industrial scale. The project, named HYFLEXPOWER, is aimed at converting a 12 MW combined heat and power plant powering a pulp-and-paper industrial site in Saillat-sur-Vienne, France. Hydrogen is expected to be produced via electrolysis from surplus RES in the region and while some of it will be used for storage, the existing SGT-400 industrial GT at the CHP plant will be modified to combust a variety of natural gas and green hydrogen mixtures, working to continually raise the hydrogen fuel volume to at least 80% and eventually to 100% [44–49].

Table 1 provides a summary of the main Power-to-X (PtX) projects currently under development for use with conventional power plants, where X can represent any form of energy. Although all of these projects involve the production of hydrogen through water electrolysis, they differ in terms of their hydrogen storage solutions, power ratings, and target sectors (mobility or industry). They present a significant spectrum of size variation, from small systems with a power rating of 0.4 MWel to large hydrogen infrastructures exceeding the GW scale. Given the significant differences in size and adopted technological solutions, it is crucial to establish a common benchmark for various projects. There is a significant number of studies in literature addressing various aspects of the Power-to-X concept. Heyman et al. [58] present a flexible framework for comparing the performance of PtG sites, providing useful indicators for energy conversion technologies, plant size, cost structure, and configuration. Crespi et al. [59] compare the use of hydrogen-based systems, battery systems, and hybrid hydrogen-battery systems to meet a constant 1 MWel demand with electricity from a dedicated photovoltaic plant. In this case, systems are designed with the objective of minimizing the annual average cost of electricity. In another study, Loisel et al. [60] conduct an economic evaluation to predict the LCOH for different scenarios. The authors conclude that, for the different cases considered, LCOH would fall in the range between 4 €/kg to 13 €/kg. Bexten et al. [61] focus on the economic feasibility of on-site hydrogen supply for an industrial gas turbine, investigating the influence of parameters such as number of wind turbines, available electrolysis capacity and hydrogen storage size, leading to the conclusion that an economically viable solution for the case study under consideration cannot be defined. Other studies, including the work by Liponi et al. [62] have addressed the mitigation of hydrogen production fluctuation evaluating the inclusion of electrical storage systems. They addressed the problem of choosing the storage size as a compromise between the improvement of electrolyzers utilization factor and costs limitations. However, they found that minimum effective electrical storage size resulted in prohibitively high hydrogen costs.

The discussed literature review represents an important foundation for the objectives of this study, as it has allowed for a better contextualization of the analysis within the present research context and industrial development, enabling some of the initial assumptions and serving as a reliable benchmark for the obtained results. Approaching the topic from a closer and more comprehensive viewpoint, considering the entire supply chain, research on power-to-gas systems can be divided into three main categories: hydrogen production, storage, and consumption. While the use of hydrogen for the considered scope of this study has already been extensively discussed, as far as production and storage are concerned, it is important to contextualize the present research efforts. Considerable attention is currently being devoted to the direct integration of RES and electrolyzers, while hydrogen storage is investigated harnessing both traditional and innovative technological solutions.

Table 1
Major Power-to-X projects under development worldwide, readapted from Ref. [50].

Project	Location	Product	Start	Size [MW_e]	Ref.
ACES	Utah (US)	H_2	2019	1000	[51]
ROBINSON	Eigerøy (NO)	H_2, Biogas	2020	0.4	[52]
FLEXnCONFU	Lisbon (PT)	H_2, NH_3	2020	1	[53]
HYFLEXPOWER	Saillat-sur-Vienne (FR)	H_2	2020	12	[54]
Hydaptive	Ohio (US)	H_2	2021	485	[55, 56]
Green Hysland	Majorca (ES)	H_2	2021	–	[57]

1.2.1. Water electrolysis technologies

The three principal categories of electrolyzers and their salient features are presented in Table 2. Alkaline Electrolyzers (AELs) occupy a significant market share and have a long history of development. Solid Oxide Electrolyzers (SOELs) exhibit high efficiency due to their ability to split water at high temperatures while requiring less electrical input compared to the other technologies. Proton Exchange Membrane Electrolyzers (PEMELs) have experienced substantial growth in recent years with the commercialization of large-scale systems now in progress.

Some advantageous properties of PEM technology are low gas permeability, high proton conductivity, thin proton exchange membranes, and compactness. During operation, they exhibit high efficiency, high power density, fast response, low operating temperature, and simple balance of plant design [65]. Furthermore, as illustrated in the study by Van Der Roest et al. [66], the potential of waste heat recovery from large-scale PEM electrolyzers to improve overall system efficiency can be a relevant aspect to be analyzed. The authors examine different use cases representing possible scenarios for local system integration, such as delivering heat to a local district heating system. Traditionally, the heat (50÷80) °C generated by the stacks is dissipated through dry coolers, however, studies like this and the work from Saxe et al. [67] show that there is further potential to utilize waste heat also for water preheating, thereby further increasing the system's efficiency.

The average size of PEM electrolyzer installations has experienced consistent growth over the past decade and in recent years, several plants with capacities exceeding 1 MW have been commissioned. PEM electrolyzers are progressively gaining ground on alkaline technology. Currently, PEM electrolysis plants are in operation or being commissioned with capacities of up to 20 MW. In Europe, planned PEM electrolyzer projects with multi-MW capacities include REFHYNE [68] (ITM, 10 MW), H2Future [69] (6 MW), and Haeolus [65] (Hydrogenics, 2.5

Table 2
Comparison of the main characteristics of different types of electrolyzers, readapted from Refs. [63,64].

Technology	Operating temperature	Stack voltage efficiency	Pros and cons
Alkaline electrolyzer (AEL)	<80 °C	(62÷82) %	Pros: - durability - maturity Cons: - poor partial load range - low current density
Proton Exchange Membrane Electrolyzer (PEMEL)	<80 °C	(60÷80) %	Pros: - compactness - quick response Cons: - high cost - lower durability
Solide Oxide Electorlyzer (SOEL)	>700 °C	(95÷100) %	Pros: - high efficiency - heat production Cons: - low technology maturity

MW). A 20 MW PEM electrolyzer by Cummins is expected to go into operation in Canada in 2024 [70]. In the 2020-2025 period, there are several planned projects with capacities ranging from 50 MW to over 250 MW, pending final financing approval [71].

1.2.2. Storage

At present, hydrogen storage is tackled through various technologies, with the primary solutions consisting of physical storage, either in the form of compressed gas or liquid, and material-based technologies [72]. While the latter is still in its developmental stage and liquid storage is more suitable for long-distance transportation, physical storage of hydrogen in tanks through compression is the most optimal solution for large-scale production hubs, such as the one examined in this study. This approach is not only well-established due to its strong link to the natural gas industry, but also allows for a better dynamic operation of the resource with regard to filling and release procedures, thus making it more suitable for the needs of complex and dedicated hydrogen hubs in the decarbonization of energy-intensive sectors [73].

1.3. Aims and novelties

The purpose of this study is to investigate the techno-economic feasibility of decarbonizing the consumption of a paper mill through the retrofit of an existing gas-turbine based cogeneration system and the development of a dedicated hydrogen production plant that relies solely on renewable production from solar energy. In particular, the focus is on the need to study the adaptability of current energy systems to the transition to the new hydrogen energy carrier. Given the rapid and growing expansion of green hydrogen in the decarbonization of heavy industry and power generation, this paper draws on the importance of measuring the cost and performance of systems that can be rapidly converted to 'hydrogen-ready'. The retrofitting of an existing infrastructure presents a distinct advantage in terms of reduced expenditures and optimized implementation timeline, as compared to a new, standalone construction. The present work endeavours to conceptualize an innovative modelling framework that can allow comprehensive analyses of reconverting traditional power generation facilities to sustainable operations.

Starting from a set of consumption data of a paper mill facility, currently satisfied by conventional natural gas-fuelled CHP technology, the retrofit of the system for hydrogen operation has been modelled in detail using different dedicated numerical tools. Characterisation first involved the construction of a traditional cogeneration system model, which has been subsequently modified to consider hydrogen as a fuel. Based on the derived results, a dedicated hydrogen production and storage plant is then dimensioned to meet the fuel demand. Thus, by making the different energy models and flows interact, annual simulations are carried out on an hourly basis evaluating all the possible combinations of different sizes of photovoltaic field and electrolyzers in order to define an optimal solution from a techno-economic standpoint. It must be specified that the solution defined as best results from a simulation-based approach rather than the application of a specific optimization algorithm, and it is this that is referred to as 'optimal' in this study. A detailed explanation is provided in Section 3.2. Finally, economic sensitivity analyses are carried out to assess the performance of key indicators such as LCOH and Net Present Value (NPV) considering different energy market scenarios.

In innovative terms, this study intends to offer a novel perspective on the adaptation of traditional utility-scale systems to renewable fuels as a trade-off between the exploitation of already existing and valuable infrastructures and the acceleration of the transition towards the total decarbonization of energy systems. Based on the most recent industrial developments and launched flagship projects (as presented in Table 1), it precisely defines the performance of a retrofitted GT-based system and indicates its potential and operability limits for the envisioned application. To the best of the authors knowledge such models are still little discussed in the literature at this level of detail and this study contributes both in terms of methodology and results to their analysis.

Moreover, in contrast to many of the Power-to-Power (PtP) system studies present in literature, this work accounts for the implementation of detailed realistic technologies models and how their performance influences the optimal layout solutions in the context of fluctuating hydrogen demand and renewables production. By developing a dedicated simulation framework, this work also aims to present a flexible techno-economic model for the production, storage and consumption of electrolytic hydrogen in a scenario with fluctuating demand and an innovative cogeneration system. The model is then applied to simulate a large number of hydrogen production plant combinations, presenting its flexibility in testing a wide range of different configurations over extended periods of time to assess long-term performance and optimise components' capacities and operations. As further discussed in the dedicated section, its open-source nature encourages collaboration, knowledge sharing, and further advancements in the field of hydrogen production and renewable energy integration.

One of the main objectives of this analysis is to examine the thermodynamic principles of each process along the hydrogen value-chain, with the goal of characterizing the energy performance while providing a reliable methodology for modelling and simulating green hydrogen industrial hubs. This enables an accurate calculation of the system overall energy performance, yielding all relevant data for the comparison of various decarbonization solutions in similar contexts. Moreover, the evaluation of key techno-economic parameters provides valuable insights for short- and long-term investment and policy planning for the adoption of hydrogen in industry.

In order to address the presented purposes, the paper has been organized as follows. Section 1 provides a comprehensive literature review of PtP systems, technologies and case studies, presenting the work from the perspective of the gap it aims at filling in the existing body of knowledge. Section 2 after the description of the case study, provides exhaustive specifications on the techno-economic principles and methodology adopted for the simulation of each involved system. Section 3 outlines and discusses the main results of the energy balance analysis identifying the optimal configuration definition based on the results derived from the CHP system simulation. Major findings and sensitivity analyses are presented and discussed in light of both economic and sustainability terms. Finally, in Section 4, the main observations and conclusions are outlined.

2. Materials and methods

2.1. Reference case study

The considered case study focuses on a paper mill plant located in Europe, with electricity and steam consumption data provided for one year of operations. The heat demand is represented by saturated steam at a constant pressure of 20 bar for the process needs. As a baseline-scenario overall energy demand is covered for the most part by a traditional GT-powered CHP system fuelled with Natural Gas (NG). The cogeneration systems consist of a gas turbine which produces electricity that directly supplies the facility request. The exhaust gases from the turbine are then directed to an HRSG which recovers the thermal energy necessary to produce the required process steam. The feasibility of converting the combined heat and power system to run on locally produced green hydrogen, via designing an optimized production and storage system combination, is evaluated in this study from both a technological and economic perspective.

2.2. Data analysis

A thorough analysis of the consumption data of the industry under examination is of paramount importance for the proper modelling and sizing of the CHP plant. The electrical consumption is relatively stable

throughout the year, while the steam demand of the utility is characterized by greater fluctuations. The demand profiles for both electrical power load and steam request can be converted into cumulative curves, as presented Fig. 1. Such curves are obtained by ordering the hour-by-hour demand values from highest to lowest. A brief analysis of the data allows for the identification of key characteristics of the resulting curves, which are listed in Table 3.

Major indicators are presented such as maximum, minimum, and mean values for both electric load and required steam mass flow rate. Additionally, values observed in correspondence of ¼ and ¾ of the operating time are shown. Among the presented values, a key factor in the design of a dedicated cogeneration plant is represented by the maximum rectangular area enclosed by the combined cumulative curves, both for thermal and electricity distribution curves. A common approach in the dimensioning of a CHP system is in fact the Maximum Rectangle (MR) method [74,75]. The MR method, as opposed to other optimization techniques, prioritizes identifying the most efficient capacity of an energy generator, one that can satisfy a significant proportion of energy consumption, rather than solely targeting the maximum demand. Once the cumulative curves have been generated, via the MR method the rectangle which has the maximum area is detected, its height representing the theoretical highest capacity of the generator. This approach generally yields a superior benefit-cost ratio for energy systems, as it aims to determine the optimal size of the CHP system that can meet the majority of energy consumption.

Building on this approach the selected rated power of the generator will be slightly higher than the one maximizing the energy provided at full load, as a widespread sizing approach indicates [76].

Given the strong dependence between weather data and the performance of the cogeneration system, it is necessary to consider environmental factors in subsequent modelling analyses. Therefore, the ambient temperature profile for the hypothetical site being examined, based on the reference year, was retrieved from a database available at [77] and is shown in Fig. 2.

2.3. CHP system modelling

Before going into detail with the simulation procedure, it is necessary to describe the cogeneration plant under consideration. A schematic plant scheme is presented in Fig. 3.

Ambient air flows into the compressor (1) before entering the combustion chamber (2) where it reacts with the fuel before expanding into the turbine (3) and producing electricity. The exhaust gases then flow into the evaporator (7) and economizer (5) section to exchange heat with the water-steam circuit, before being released into the atmosphere at the stack (10). Contemporarily, condensed water returning from the process at a pressure of 101325 Pa and a temperature of 30 °C is pumped

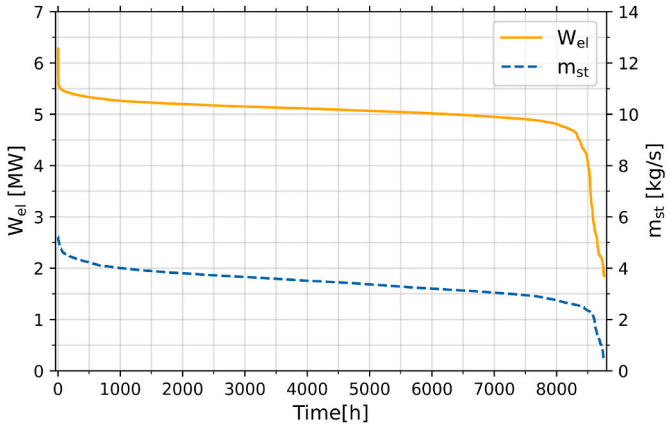

Fig. 1. Cumulative curves for steam and electricity request.

Table 3
Data descriptors of cumulative curves.

	W_{el} [MW]	m_{st} [kg/s]
Maximum	6.27	5.22
Minimum	1.84	0.37
Mean	5.01	3.42
¼ (2190 h)	5.18	3.76
¾ (6570 h)	4.97	3.11
Max area rectangle	4.68[a]	2.89[b]
Standard deviation	0.44	0.56

[a] In correspondence of the 8246 h.
[b] In correspondence of the 7689 h.

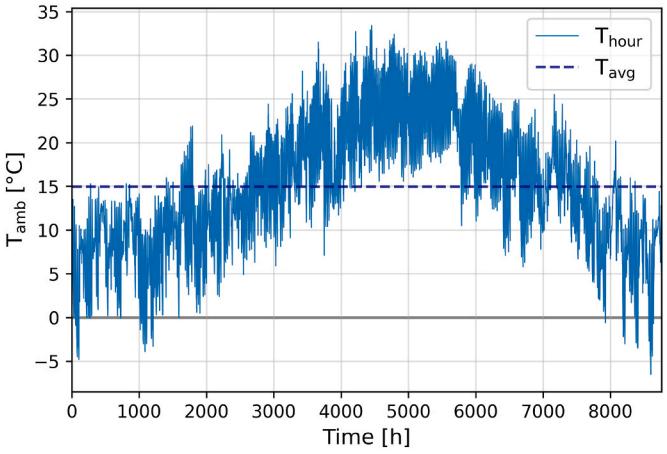

Fig. 2. Hourly ambient temperature profile for the considered location.

(4) at a pressure of 20 bar. After crossing economizer (5) and diverter (6) sections, water at a temperature of 10 K lower than T_{sat} is sent to the boiler drum (8). It is crucial to maintain a temperature differential of ΔT_{sub} above 0 K to prevent boiling inside the economizerpipes. In the boiler drum, subcooled water is combined with saturated steam originating from the evaporator. The residual liquid fraction is then redirected to the inlet of the evaporator via natural circulation where a portion is transformed into steam before being reintroduced into the boiler drum. The temperature difference between the flue gas and steam at the inlet of the HRSG is known as the approach point temperature difference (ΔT_{app}), while the temperature difference at the outlet of the evaporator is referred to as the pinch point temperature difference (ΔT_{pp}). The latter parameter plays a crucial role in the design of the HRSG, as it determines the required heat exchange area and subsequently the cost of the system. Located immediately downstream of the turbine, the bypass component enables a portion of the flue gas mass flow to be discharged directly into the atmosphere, bypassing the HRSG. This results in a reduction in the amount of steam produced by the waste heat boiler. A much more comprehensive description of the presented components can be found in Ref. [78].

Based on the data analysis presented in Section 2.2, a specific gas turbine model was chosen from the commercially available options, with consideration given also to its readiness for hydrogen fuelling. The aforementioned, is the first necessary step in the direction of modelling (i.e. designing) a GT-HRSG coupled cogeneration system capable of satisfying most of the facility demand, according to the presented MR approach. Therefore, a SGT-100 gas turbine produced by Siemens [79] with a nominal electrical power output of 5.4 MW (shaft power, ISO ambient conditions), 30.1% gross efficiency and an exhaust mass flow of 21 kg/s at a temperature of 549 °C has been considered as a starting point for the analysis. To date, the H_2 co-firing capabilities of this turbine, allow for up to a 65% blend in volumetric terms.

The aim of this analysis is to reliably predict the operation of such a

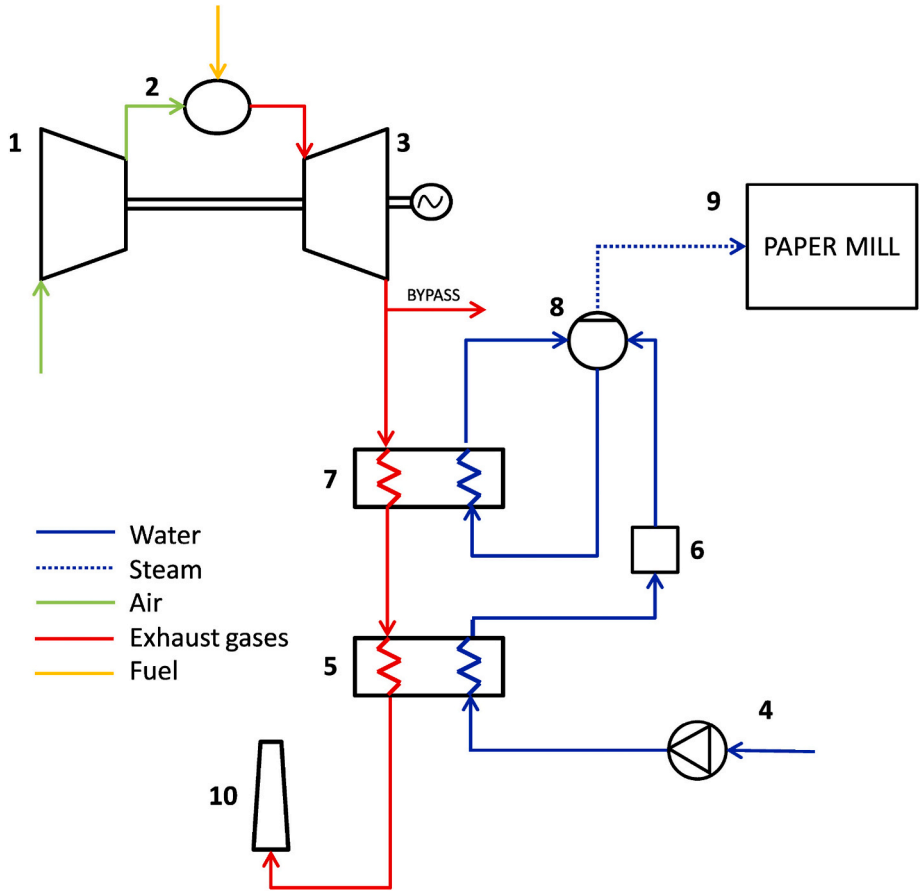

Fig. 3. Schematic diagram of the considered cogeneration plant.

system when fuelled with a 100% renewable hydrogen fuel stream. In pursuit of this goal, after the modelling of the baseline NG scenario, the system has been assumed to work with minor adjustments in the combustion chamber, thus allowing for the functioning with pure hydrogen.

A detailed model of the presented CHP system has been developed and specifically adapted to work with hydrogen using the Energy System Modular Solver (ESMS) modular tool. The paramount feature of this modular simulation software is the capability of analysing different power plant configurations without generating an additional source program. Irrespective of their level of complexity, cogeneration plants can always be broken down into a finite number of recursive components (turbines, pumps, heat exchangers, valves, etc.), their scheme (however complicated) is examined as a system of n equations in n variables linked together through thermo-fluid dynamic relations. Each module is described as a black box able to simulate a set of desired chemical and thermodynamic transformations. The resulting series of non-linear equations identifying the power plant is afterwards linearized, while the coefficients are constantly updated during the program execution. All equations are then solved simultaneously using a classic matrix method utilizing a fully implicit linear approach. The reader is referred to Refs. [80–84] for a detailed description of the code and the entire set of thermodynamic equations used in system configurations like the one presented in this study and many other engineering applications.

2.3.1. Simulation procedure

The simulation procedure is divided into two distinct and consecutive steps. The first phase involves creating a virtual twin model of the selected cogeneration technology. Considering the conventional natural gas-fuelled operation, a design point for the GT-HRSG system has to be defined to establish the geometries of the different components. Therefore, based on the technical data provided by the manufacturer, a specific GT model was created and simulated to evaluate its performance and define the geometry of the cogeneration system in its entirety. The second step uses the defined geometry as an input to calculate the performance in off-design conditions, considering hydrogen to be fed to the combustion chamber.

The overall procedure is presented in detail in Fig. 4. The procedure starts by evaluating the performance of the gas turbine under design ambient conditions and full load. The design points are based on standard ISO conditions (P_{ISO} = 101325 Pa, T_{ISO} = 15°C, x_{ISO} = 60%, etc.). Once obtained the thermophysical properties of the flue gases, they constitute the input data set for HRSG dimensioning, together with the required steam flow properties (P and vapor fraction), the pinch point temperature difference (ΔT_{pp}) and the sub-cooling temperature difference (ΔT_{sub}). Based on the considered application, the design steam output resulted in 3.97 kg/s. After establishing the set of boundary conditions, it is possible to proceed with the design of the HRSG by determining its geometry. This design is then used as a fixed parameter for subsequent simulations of off-design conditions.

Table 4 presents the results obtained via the modular code, which allows the user to determine the characteristic parameters of the commercial gas turbine based on the manufacturer datasheet. It is thus possible to visualize the main output obtained for the system running both on natural gas and hydrogen, and to make a comparison with manufacturer data to validate the procedure.

As the data showed good agreement, it has been possible to proceed with the construction and simulation of the hydrogen-fuelled case, also presented in the table. Once the model was modified to incorporate the use of 100% hydrogen, the definition of the heat recovery system capacity was enabled, determining the amount of steam that can be generated under ISO conditions.

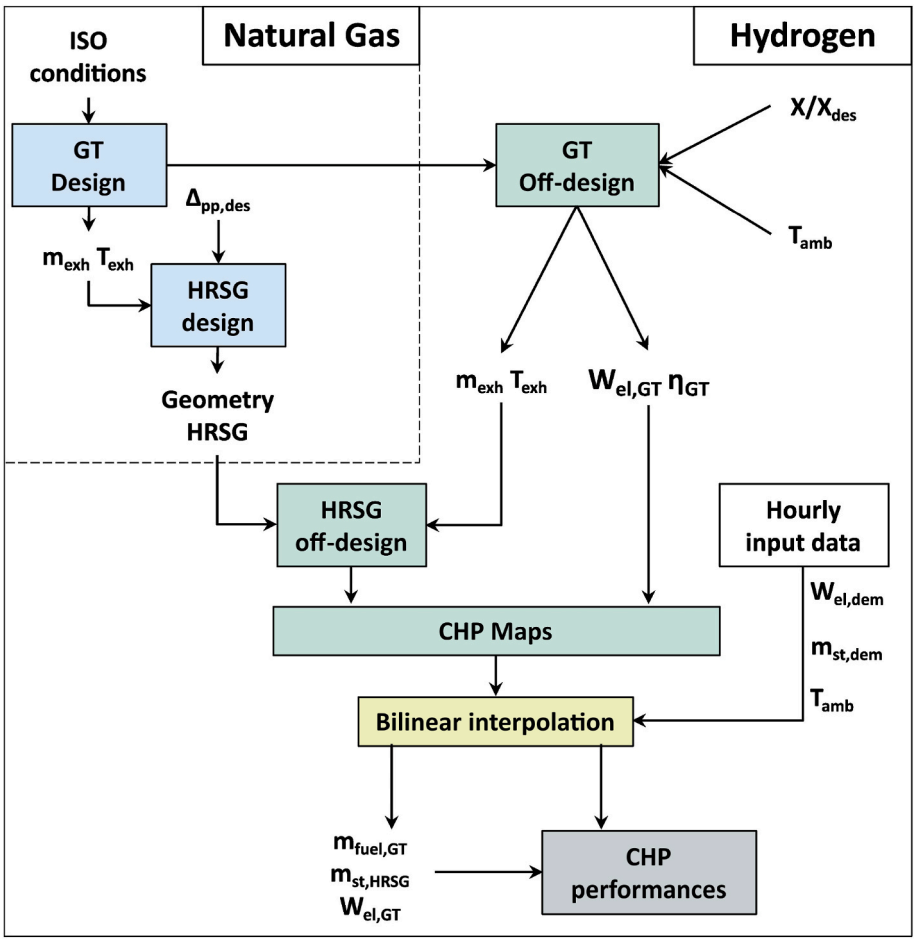

Fig. 4. Schematic flowchart of the adopted simulation procedure.

Table 4
SGT-100 turbine performance, compared to ESMS code results.

	Units	Datasheet	ESMS	
			Natural Gas	Hydrogen
Output power	[MW_{el}]	5.4	5.4	5.649
Gross efficiency	[−]	0.302	0.303	0.311
Heat rate	[kJ/kWh]	11,913	11,881	11,562
Pressure ratio	[−]	15.6:1	15.6:1	15.62:1
Exhaust mass flow	[kg/s]	21.0	20.999	20.764
Exhaust temperature	[°C]	549	549	548.683

The visualization provided in Fig. 5 confirms the validity of the sizing choice as the system can cover most of the operating points, both thermal and electric, even when operating at partial-load. From the perspective of power consumption, electrical and thermal loads tend to fluctuate over time; on the power production side, environmental conditions also tend to vary.

Thus, it is essential to evaluate the performance of CHP plants taking into account the off-design conditions of both GT and HRSG. One of the primary goals of the current research is to consider both the design and off-design effects in the simulation of the presented CHP plant operating on green hydrogen, in order to accurately quantify the necessary fuel consumption, and subsequently, to design the dedicated e-fuel production and storage system upstream of it.

The off-design simulation procedure is initiated with the simulation of the gas turbine. The boundary conditions remain consistent with those established by ISO standards, except for the temperature, which is considered based on the range variation observed at the site (see Fig. 2).

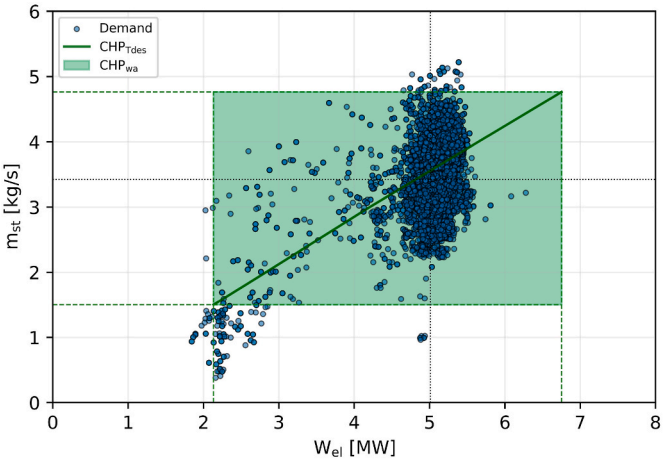

Fig. 5. CHP system working area for ISO conditions against hourly facility needs throughout the year.

The power output, given as input of the simulation, is varied in a span comprised between 20% and 30% of the rated power output, which for the case of the H_2-fuelled gas turbine is 5.65 MW while the Turbine Inlet Temperature (TIT) is always kept below 1530 K. For each step of the considered interval, the off-design performance of the turbine is calculated, and the results of this simulation are provided as input to the HRSG model to define its behavior under off-design conditions. The most relevant outputs of this procedure are GT efficiency (η_{GT}), the

turbine power generation ($W_{el,GT}$) and mass flow rate (m_{exh}) and exit temperature (T_{exh}) of the exhaust gases. This set of values, along with the hourly steam mass flow demand and the pre-calculated HRSG geometry, serve as input parameters for simulating hourly off-design scenarios of the HRSG. The resulting outputs, including the TIT and Stack gas Temperature (ST), are used to calculate the system operating maps while adhering to its specific technical operational limitations. These maps are then queried to simulate the system actual performance in a thermal load-following mode at each hourly timestep. The inputs used to query the maps are the hourly steam demand ($m_{st,dem}$) and ambient temperature (T_{amb}), which, intersected as lookup keys through bilinear interpolation of the previously generated data sets, yield parameters of interest such as hydrogen consumption ($m_{fuel,GT}$), produced steam ($m_{st,HRSG}$), and turbine electricity output ($W_{el,GT}$). The operational strategy adopted is built around a nominal steam mass flow rate produced by the HRSG of 3.97 kg/s. Such output is subjected to substantial fluctuations resulting from the various working conditions encountered during annual operation, which establish upper and lower operating limits at each timestep. If the steam mass flow rate falls below the lower operating limit, the diverter is activated to directly discharge part of the flue gases in the environment bypassing the HRSG and thus allowing the system to meet the punctual demand of the facility. In contrast, to achieve a steam mass flow rate higher than the maximum operational output, a hydrogen-powered Steam Generator (SG) has been considered in support of the cogeneration system, as shown in the overall plant diagram in Fig. 7. This SG has a nominal capacity of 3.5 MW and is capable of supplementing steam production if the GT cannot meet the full thermal energy demand. This decision was made with the aim of maintaining a system powered by 100% renewables, taking into account the early stage of the technology maturity, although the first commercial applications for the paper industry are already available on the market [85,86].

In Fig. 6 the behavior of the cogeneration system components is represented in response to the total thermal power demand of the facility. Thresholds are depicted based on this demand, which illustrate the two different system operating modes. Point 'a' represents the cut-off value below which the GT can meet the thermal demand by operating at minimum load utilizing the bypass valve to divert some of the exhaust gases. From heat demand defined in point 'b' onwards the GT operates at its maximum load and the remaining unmatched demand is covered by switching on the auxiliary SG. The thresholds depicted in Fig. 6 are purely illustrative, as they depend on the specific thermal power demand, inlet air temperature, minimum permissible GT load (GT_{min_load}), and maximum bypass duct opening and may therefore fluctuate based on the prevailing conditions at any given time-step. The HRSG can satisfy steam mass flow demand throughout the year by using the flue gases diverter or the additional SG during off-design conditions. In some cases, the power generated by the turbine may not meet or exceed the power requirement of the utility, however, the plant is considered to be connected to the grid, allowing the system to be always balanced by supplying or injecting electricity respectively from or into the grid. As a main indicator of the CHP performance the global first principle efficiency has been chosen. This is considered as a gross indicator of the global efficiency of the system and is defined as the ratio between useful power (both thermal and electrical) and the energy consumed via burning the fuel in GT combustor. It is defined as [87]:

$$\eta_{tot} = \frac{W_{el} + Q_{CHP}}{Q_{fuel}} \tag{1}$$

Where W_{el} is the electricity produced by the cogeneration system, Q_{CHP} is the thermal energy recovered by the HRSG and Q_{fuel} is the chemical energy contained in the fuel entering the combustion chamber.

2.4. Hydrogen-integrated multi-energy system

As mentioned in the previous section, the thermodynamic analysis of the cogeneration system is crucial for investigating the feasibility of a fully integrated power-to-hydrogen-to-power system at industrial scale.

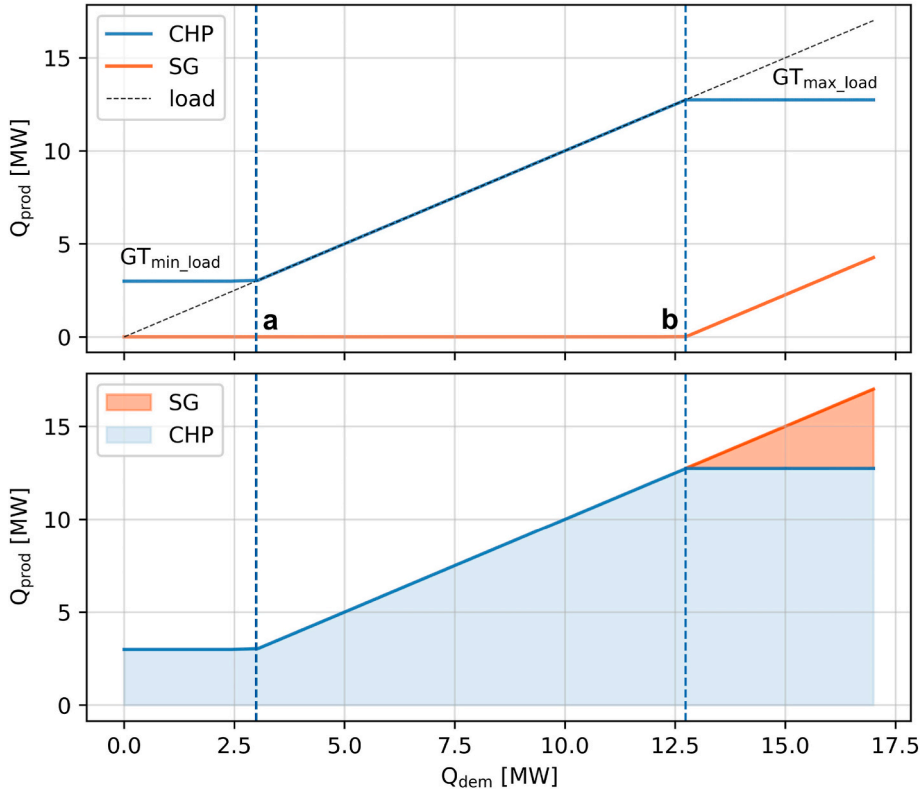

Fig. 6. Illustrative representation of the chosen system control logic.

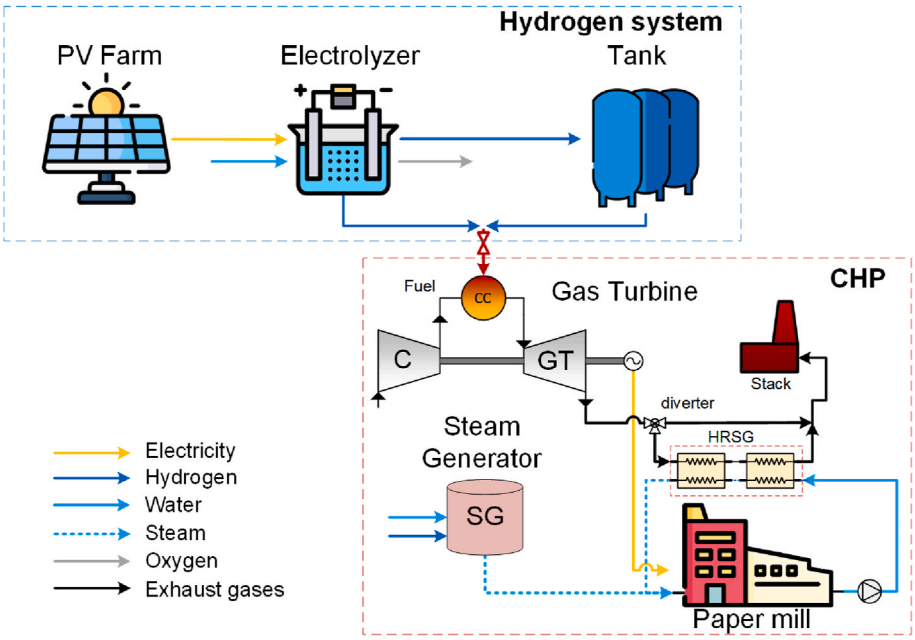

Fig. 7. Overall multi-energy system scheme.

This paragraph is aimed at presenting an overall scheme of the plant and the methods used in the modelling of its techno-economic performance. Fig. 7 illustrates the systems considered for hydrogen production, storage, and consumption for the industrial application under analysis. The proposed hybrid power plant is meant to provide electrical and thermal energy to the paper mill facility by satisfying the green hydrogen demand of the CHP system during its continuous (24 h per day) yearly operation. The system is composed of a PV farm connected to a stack of electrolyzer modules, and a tank storage system downstream of it. When solar radiation is available, photovoltaic energy is supplied to electrolyzers according to the hydrogen-driven operation mode [88]. The generated renewable electricity is firstly directed to cover the maximum electrolyzer capacity, while the remaining electricity is conveyed either to cover the remaining request of the facility or sold to the grid. Given the system operation in thermal-load follow mode, the highest priority is given to meeting the steam demand of the paper mill. According to the assumptions made, to meet the required thermodynamic conditions (P = 20 bar and T = 212 °C) for steam generation, it is necessary to use hydrogen-based systems such as the gas turbine and boiler. Electrically driven technologies, such as industrial-scale heat pumps, still face significant challenges in attaining the presented conditions of the saturated steam. Consequently, the plant adopts a hydrogen-first approach, prioritizing hydrogen production. The produced hydrogen is then stored via a multiple-tank system, from which hydrogen is directed to fuel the GT according to the hourly demand. In case of energy shortages or surplus production of electricity, the system can interact with the grid and exchange energy as needed.

2.5. Multi-energy system simulation

The energy system model utilized in the simulations of the system under investigation is the Multi-Energy System Simulator (MESS), an open-source computational modelling tool designed for analytical purposes as described in Ref. [89]. For more information on the structure and simulation logic of MESS, the reader is referred to Refs. [90,91].

For the purpose of this study, the authors have developed and integrated a dedicated simulation framework into MESS to accurately estimate the capabilities of the hydrogen production system for industrial applications. Hydrogen-related technologies models have been therefore expanded and adapted to assess the decarbonization potential for green hydrogen in energy-intensive industries. The modelling approach adopted for these components is described in more detail in the following section. The management of power fluxes at each time step is modelled as follows. Regardless of systems size, initially, photovoltaic production is considered to be fed to the electrolyzers stack up to their maximum capacity in case enough energy is available. The solution strategy then depends on the power balance, if it is zero, the simulation continues with the following time step. If it is still positive after the electrolyzers consumption, excess energy it is either fed into the facility to compensate for any shortfall in the cogeneration system or sold to the electrical grid. On the other hand, if the power balance is negative after considering photovoltaic production and electrolysis and facility power demand in sequence, a similar solution process is followed, with the only difference being that the remaining power imbalance is balanced by purchasing power from the grid.

With regards to hydrogen balances, the resulting output from electrolysis conversion of renewable power updates the tank State of Charge (SOC) at the considered timestep. Thereafter, accounting for the demand required by the gas turbine SOC is furtherly updated by subtracting the required hydrogen amount. The power and hydrogen balances are updated accordingly. The time step considered for the analysis is 1 h, and demand profiles have been aggregated consequently.

2.5.1. PV production

To accurately estimate the producibility of green hydrogen in one year of operation, solar energy production potential for the selected location has been retrieved from MERRA-2 database [77,92].

Normalized data production with hourly temporal resolution have been fed as input to the simulation to initialize the energy balances at each timestep. In Fig. 8 daily average photovoltaic production is presented as a means of visualizing the trend distribution over the year. A significative increase is observed during the summer months compared to a relatively stable hydrogen demand of the cogeneration system. The solar output is represented as the ratio of energy produced to the rated power of the renewable energy system, taking into account both day and night hours. This is because it is the sole source of green hydrogen production for the continuous operation of the paper mill. The representation highlights the mismatch between the generation and demand of the electrolyzers and provides a first qualitative measure of the significant seasonal storage capacity required.

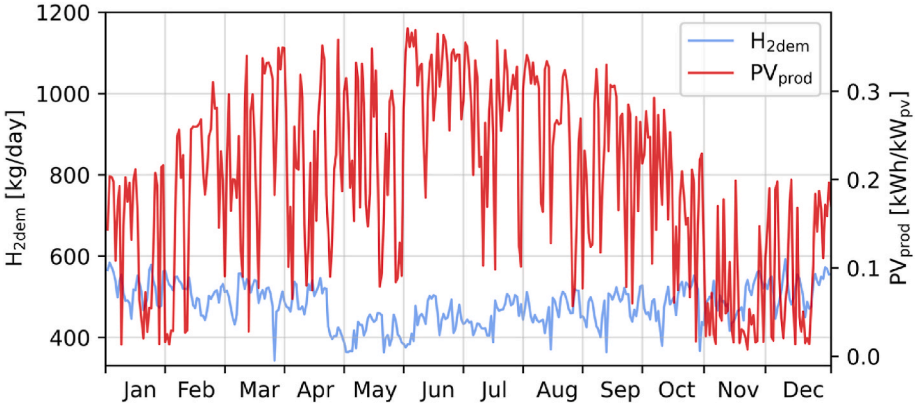

Fig. 8. Solar photovoltaic production for the considered location and paper mill hydrogen demand.

2.6. Models

As in the nature of the modular approach standing at the core of the simulation tool, a library of predefined technologies is available for the user to build a wide range of different case studies. Once the main structure of the system has been defined by the user, the simulation of the energy balances is initialized. Adhering to an Object-Oriented Programming approach, each technology model can be invoked and executed from the main program at each time step, producing thermodynamic outputs that depend on specified inputs such as available energy flows and weather conditions.

2.6.1. Electrolyzer

For the considered case study PEM electorlyzers have been selected to assess the hydrogen production capabilities. The reasons behind this choice are the advantageous features of rapid response to photovoltaic power generation, high product purity (hydrogen and oxygen as by-product) and a good compromise between cost, efficiency, high current density, and low operating temperatures [93,94]. A detailed model of a PEM electrolyzer has been developed by the authors and a thorough description of it can be found at [91].

The model has been developed to accurately simulate the real-world operation of such complex system. Some important properties of the considered electrolyzer are presented in Fig. 9. The polarization curve shows the relation between current density and stack potential, taking into account various losses, as it is a common approach in modelling the physic of electrolysis [63,95,96] as demonstrated by Eq. (2).

$$V_{stack} = N_{cell}(E_{cell} + L_{act} + L_{ohm} + L_{con}) = f(i) \tag{2}$$

Where N_{cell} represents the number of cells, E_{cell} is the open circuit potential, L_{act} is the activation overpotential, L_{ohm} the overpotential due to ohmic resistance, L_{con} the concentration overpotential while i is the current density flowing through the cells. The obtained set of points is then interpolated using a linear spline function to allow for each time-step to compute the exact functioning point of the electrolyzer when queried with the electric energy from the PV farm. As a result, the key operating parameters, such as hydrogen production and electrical efficiency, can be calculated within a range of operations that spans from 10% to 100% of the nominal power of the electrolyzer, since the stack does not operate at constant power but is subjected to the fluctuation of renewable power production. A decision was made to not operate the electrolyzer below 10% of its rated power due to reasons related to low conversion efficiencies. Excess heat from the operation of the electrolyzers is supposed to be dissipated via dry coolers.

The PEM electrolyzer units modelled in this study consist of modules of 1 MW of rated power, characterized by an electric efficiency of approximately 60%. This parameter can be converted in a power-to-gas conversion factor indicating the amount of hydrogen produced by the electrolyzer per MWh of input energy, equal to 17.5 kg/MWh which is a value in line with the current literature and models available on the market [65].

For the purpose of this study, different sizes of electrolyzer stack made of 1 MW modular elements are considered for green hydrogen production. At every timestep, the electrolyzers system is queried and modules are activated in sequence according to the available energy (if above the activation threshold) until all installed modules are turned on in parallel when the generated power peaks exceed the installed capacity. Fig. 10 gives an illustrative representation of the operation logic of the installed electrolyzers stack.

At the end of the one-year-long simulation, the cumulative H_2 output provides a precise evaluation of the annual hydrogen production capacity of the system.

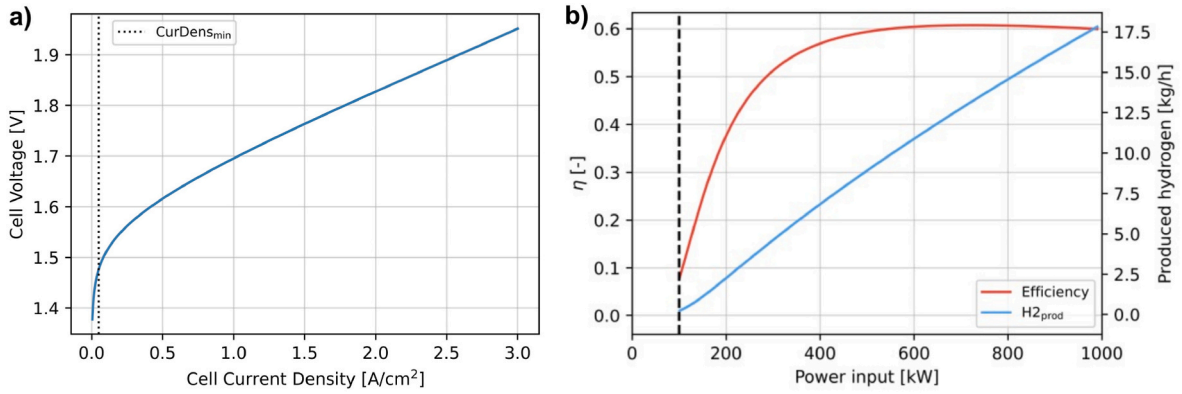

Fig. 9. Electrolyzer model main outputs: single cell polarization curve (a), efficiency and hydrogen production varying power input for a 1 MW module (b).

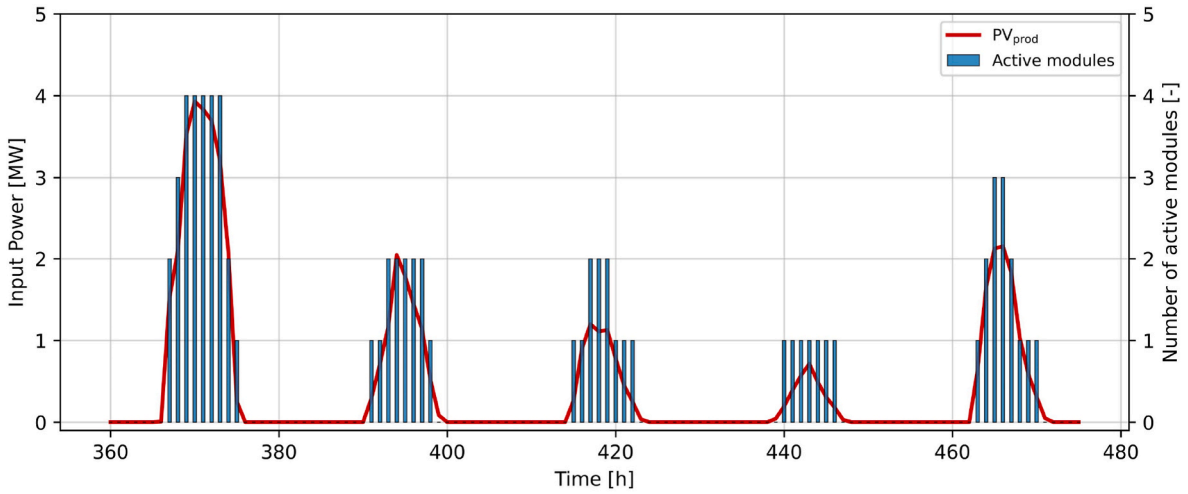

Fig. 10. Illustrative representation of electrolysis plant operation. System size: 4 MW of electrolyzers and 6 MW of PV capacity.

2.6.2. Storage system

It is essential to consider a seasonal storage system, capable of absorbing the fluctuations in renewable production and ensuring the continuous operation of the paper mill throughout the year. All the hydrogen consumed by the CHP has to be produced on-site and no external supply system has been envisaged. It is important to emphasize that the hydrogen demand must be met even during night-time hours when the renewable production is not available, reasonably entailing an increase in storage system capacity compared to a continuous operation of the electrolyzers.

The produced hydrogen is stored in a system of tanks at a pressure of 30 bar, equivalent to the pressure at which hydrogen is released from the electrolyzers without the need for further compression. The storage pressure value for hydrogen has been selected in accordance with other relevant studies [97,98]. Even for real-world large-scale projects such as the one commissioned by Iberdrola in Puertollano [99] (the largest green hydrogen plant for industrial use in Europe), above-ground storage in the form of compressed gas in tanks at a pressure of 60 bar is considered for a total of around 80 t of hydrogen. As a result, for the purposes of this analysis, no further compression was considered, adopting a simple tank model that allows the quantification of the amount of hydrogen flowing within a hypothetical tank system, allowing the correct sizing of the system in terms of mass capacity. In order to minimize the volumetric storage footprint, other solutions such as high-pressure compression, underground storage or hydrogen liquefaction should be evaluated, but this has not been considered in this study.

The State of Charge (SOC) of the storage system is updated at each time step by the model through the calculation of the simultaneous balance of hydrogen production and demand. The chosen approach is dynamic and initially allows the stored hydrogen level to freely oscillate between positive and negative values throughout the simulation year, then shifted to positive values to align the minimum with a SOC of 0%. This model is valid within MESS both in the case of optimal sizing of the tank system and in the case of fixed sizes.

As an example of the operating logic of the tank model and the influence on the system of the variability of the renewable resource under the same hydrogen demand and system configuration, Fig. 11 is presented. The evolution of the state of charge of the storage is shown for plant configurations of the same size yet located at two different sites, one with a temperate oceanic climate (Oslo) and the other with a Mediterranean climate (Palermo). In this case, a 155 MW photovoltaic plant, a 100 MW electrolyzer stack and 100 t tank capacity are considered. Given the same end-user demand for green hydrogen, it is interesting to visualize how the effect of different availability of the solar resource during the year affects the overall system balances. The specificity of the climate at the two different sites is reflected in a greater capacity factor and utilization of the resource when solar energy availability is higher.

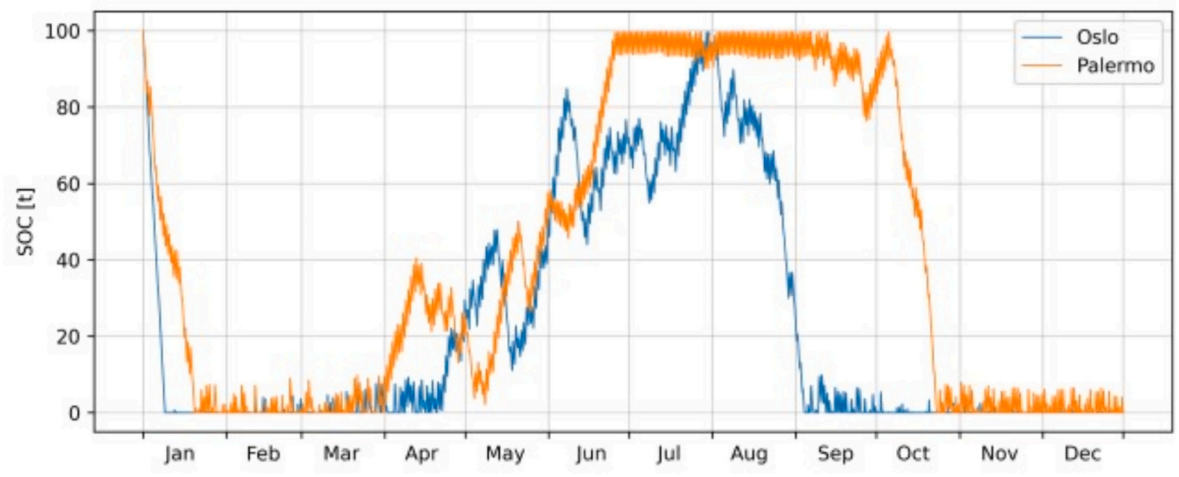

Fig. 11. Hydrogen tank SOC trend for two different locations for a system consisting of a 155 MW PV plant, 100 MW of electrolysis power and 100 t of storage capacity.

2.7. Sizing

In this section, the approach used in sizing of the hydrogen production system is explained. To calculate the optimal configuration of the system, considering on-site production of hydrogen, it was necessary to simulate various combinations of electrolyzers, storage systems, and PV farm capacities and to assess their performance over the year. The initial step was to define a suitable range of sizes for both the rated power of the photovoltaic field and electrolysis capacity, consistent with the scale of the problem under consideration and focused on hydrogen production capability. Following a general grid-search approach [100], (0÷300) MW and (40÷90) MW of solar and electrolysis capacities respectively were combined and simulated pairing each PV value with the entire spectrum of electrolyzer sizes. Hydrogen production capacity is evaluated for each combination by assessing on an hourly basis the solar energy available that can be converted by the electrolytic system, considering the operational curves, working limits, and number of modules in the stack that are activated accordingly to the available energy in that timestep. Annual production is then determined as an output for each capacity combination, resulting in a grid of n x r values, where n and r represent the array lengths for the PV and electrolyzer sizes, respectively. Based on the set of outputs obtained for the given ranges and considering the hourly hydrogen demand, all the system configurations (including tank size) capable of meeting the specific requirements of the case study are defined as follows.

The approach used in this study involved defining the objective function $f(n_{ele})$ dependent on the electrolyzer capacity as the difference between the global hydrogen demand H_{dem} and the production H_{prod} for the considered period, as follows:

$$f(n_{ele}) = \sum_{i=0}^{N} H_{dem}\,(i) - \sum_{i=0}^{N} H_{prod}(i) = 0 \tag{3}$$

where n_{ele} represents the number of electrolyzer modules (i.e., their capacity), $H_{dem}\,(i)$ represents the hydrogen demand at time i, and $H_{prod}(i)$ is the production of electrolyzers at the same timestep. The condition imposed in Eq. (3) is strict and has been verified by all combinations of photovoltaic panels and electrolyzers capable of meeting the paper mill hydrogen demand annually. For a given PV field size the electrolyzer capacity necessary to satisfy the above-mentioned condition is obtained via solving a non-linear system of equations through Newton-Raphson method [101]. An initial guess, derived from the preliminary analysis, is provided for the solution to iteratively find the root (or roots) that best approximate the real solution of the system. Iterations proceed until a satisfactory level of accuracy is reached, or until a specified maximum number of iterations is exceeded. Balances are again carried out on an hourly basis for each of the size combinations considered and the tank volume is dimensioned downstream of the sizing of the first two components. Compliance with the condition therefore requires that the tank level at the start hour corresponds to the level at the final timestep and that there is no hydrogen deficit at the end of the simulation period. This method allows a set of possible solutions to be defined among which the optimal one is then chosen based on the best overall techno-economic performance. Despite the absence of dedicated optimization algorithms, the parametric simulation approach described ensures the validity and generalizability of the results. The model is adaptable to a wide range of case studies, since the system size is provided as input and the simulation allows the evolution of results to be evaluated as different input parameters change. System performance can be defined at any point in the chosen domain, making it easier to identify any minimum or maximum points that are of major interest for analysis. In addition, the adoption of a simulation model, such as the one used in this study, makes it possible to implement detailed physical models of technologies that can more realistically predict the operation of the real system at each timestep, considering both the operating curves of individual components and the influence of the mutual interaction of different energy and material flows. Results are presented in detail in Section 3.2.

2.8. Economics

When evaluating multi-energy systems with regard to the production of green hydrogen, current literature typically employs two key metrics, namely the LCOH and the Net Present Value (NPV). These parameters can be employed in conjunction to highlight various aspects of interest for evaluating the techno-economic feasibility of the investment as indicated in studies [38,102,103]. In addition to these parameters, the Payback Period (PBP) and the Profit Index (PI) indicators, presented in this section, were also taken into account.

The NPV is the primary and most comprehensive metric for evaluating the viability of a business venture. It accounts for devaluation of currency over time by evaluating all future net cash flows generated by the project and determining the present value of the project over its lifespan. The NPV is calculated by dividing each expected future cash flow by a discount rate and then summing the results, as presented in Eq. (4)

$$NPV = \sum_{i=0}^{N} \frac{CF_n}{(1+r)^n} = \sum_{i=1}^{N} \frac{CF_n}{(1+r)^n} - I_0 \tag{4}$$

Where N is defined as the duration of the project in years which is 20 years for the case study, CF_n is the net cash flow for year n of operation, I_0 represents the initial investment (CAPEX) and r represents the rate used to calculate the present value of cash flows, typically falling within the (4÷-8)% range for investments in the energy field at the considered scale.

The considered cash flow can be summarized as follows:

$$CF = REV - OPEX \tag{5}$$

Where $OPEX$ represents the Operational Expenditures (OPEX) which consists of Operation and Maintenance costs (O&M) for each technology of the system and expenditures for the purchased electricity, while REV accounts for all the revenues from product sales (O_2) and savings (natural gas and CO_2) compared to the conventional natural gas operation of the cogeneration system. The Payback Period [104] defines the period of time necessary for the investment to regain its the initial costs and is defined as:

$$\sum_{n=1}^{PBP} \frac{CF_n}{(1+r)^n} - I_0 = 0 \tag{6}$$

While the Profitability Index (PI) [105] is used to measure the profitability of a proposed investment and is calculated as the ratio of the net present value to the initial investment cost. The higher the PI, the more profitable the investment is expected to be.

$$PI = \frac{\sum_{n=0}^{N} \frac{CF_n}{(1+r)^n}}{\sum_{n=0}^{N} \frac{I_n}{(1+r)^n}} = \frac{NPV}{I_0} \tag{7}$$

On the other hand, the LCOH is defined as a metric that calculates the cost per unit of hydrogen production over the entire lifetime of a hydrogen production system. It provides a means of comparing the costs of various hydrogen production methods and configurations, enabling for the evaluation of economic viability of different options. LCOH is a critical indicator in techno-economic analyses of hydrogen production systems and is widely used in the literature to evaluate the competitiveness of different hydrogen production pathways [106,107]. The value of this index represents the point at which the discounted sum of revenue equals the discounted sum of costs; if the hydrogen market price equals its levelized cost, the investor will recover the investment within the set time period [108].

Based on the given definition, LCOH is calculated in this work as in

Eq (8):

$$LCOH = \frac{CAPEX \times CRF + OPEX - REV_{H2}}{H_{prod}} \quad (8)$$

Where:

$$CAPEX = C_{PV}\xi + C_{ele} + C_{tank} + C_{rep} \quad (9)$$

$$C_{tech} = \left(tech_{ref} \times \left(\frac{tech}{tech_{ref}} \right)^{SF} \right) \times C_{unit} \quad (10)$$

$$CRF = \frac{r \times (1+r)^{N}}{(1+r)^{N-1}} \quad (11)$$

$$C_{rep} = \frac{RF \times C_{PV}\xi}{(1+r)^{PV_{lifetime}}} + \frac{RF \times C_{ele}}{(1+r)^{ele_{lifetime}}} + \frac{RF \times C_{tank}}{(1+r)^{tank_{lifetime}}} \quad (12)$$

$$OPEX = O\&M_{PV}\xi + O\&M_{ele} + O\&M_{tank} \quad (13)$$

$$REV_{H2} = O_{2\ price} \bullet O_{2\ prod} \quad (14)$$

Where the defined costs and revenues terms are employed in the numerator, in conjunction with ξ, a coefficient expressing the percentage of energy conveyed to the hydrogen production chain compared to the totality of resources in place. This term is considered to weigh the percentage of solar energy effectively sent to the electrolyzers on the total production and provide a more accurate measure of the actual cost of hydrogen per unit produced. As can be seen from Eq. (9) and Eq (12) it affects capital and maintenance costs for the PV farm alone. In order to calculate the total cost of PV, electrolyzers and tank, a Scale Factor (SF) equal to 0.95 has been used. The technologies reference size PV_{ref}, ele_{ref} and $tank_{ref}$ are respectively 1000 kW, 1000 kW and 2479 kg. The components' replacement cost has been also taken in to account considering a Replacement Factor (*RF*) equal to 0.3, as assessed in Eq. (12). The investment years (*N*) for this case study are 20. The REV_{H2} term presented in Eq (14) accounts for the revenues from the sale on the market of the oxygen derived as by-product from the electrolysis process. It is important to notice that the purchased electricity costs have not been considered in the OPEX, as well as the CO_2 savings have not been considered in the REV_{H2}, because they refer to the comprehensive analysis of CHP plant operation and not to the H_2 supply chain system. Another important parameter for the economic evaluation is the Levelized Cost Of Energy (LCOE), which is a measure of the average net present cost of electricity generation for the whole plant under consideration over its lifetime. To compute LCOE, the yearly expense of the generation of electricity is divided by the total load fulfilled. Based on the given definition the LCOE is calculated as in Eq (15) [109]:

$$LCOE = \frac{CAPEX \times CRF + OPEX}{E_{prodCHP} + E_{togridPV}} \quad (15)$$

Where $E_{prodCHP}$ is the total energy produced by the CHP plant and $E_{togridPV}$ is the PV surplus injected back into the grid. The major economic assumptions used in the analysis are given in Table 5.

Where the GT capital cost has been considered to be equal to 20% of the total one since it has been assumed that, in order to shift from natural gas to hydrogen, the only component of the gas turbine to be replaced is the combustor.

3. Results and discussion

The results are organized into two separate sections. The first section presents the results of the cogeneration system performance, while the second section provides an overall analysis of the multi-energy system designed for hydrogen generation, aimed at meeting the energy requirements of the paper mill. The main outcomes are also discussed accordingly.

Table 5
Main economic assumptions of the study.

H_2 supply chain component	C_{unit}	OPEX	Lifetime	Reference
PV	690 €/kW	1.29% I_0 €/y	25 years	[110]
Electrolyzer	650 €/kW	2.75% I_0 €/y	15 years	[111]
Tanks (30 bar)	387 €/kg	1% I_0 €/y	35 years	[97,111]
CHP component	**CAPEX**	**OPEX**	**Lifetime**	**Reference**
GT	224226 €	2% I_0 €/y	25 years	[112]
SG	699500 €	6% I_0 €/y	25 years	[113]
Energy/product stream	**Price**			**Reference**
$O2_{sold}$	0.05 €/kg			[114]
$CO2_{tax}$	0.0866 €/kg			[115]
$Electricity_{purch}$	165 €/MWh			[116]
$Electricity_{sold}$	25 €/MWh			[116]
Natural Gas_{purch}	2.3 €/Sm^3 or 265 €/MWh			[117]

3.1. CHP performance

3.1.1. Operational capability assessment

After the implementation of the hydrogen-powered cogeneration system model as detailed in Section 2.3, the operational limitations during off-design conditions throughout the year were first defined. Traditionally, the main parameters that need to be considered for this type of system include the percentage of rated power at which the turbine can operate, the stack temperature (ST) and the turbine inlet temperature (TIT). By imposing a steam flow rate value, simulations were performed over a wide range of temperatures (-10÷40) °C, while allowing the system to adjust the fuel flow rate, which has the major effect of varying TIT values and secondary, the turbine power output and the temperature of exhaust gases.

The main results of the analysis are presented in Fig. 12, for each of the parameters of interest, the trend was plotted as a function of ambient temperature, then comparing the results with the imposed technological limits. The load percentage was varied between 30% and 120% of the turbine rated power, whereas an upper limit of 1530 K was imposed for TIT. As for T_{stack}, a minimum exhaust gas temperature of 363 K at the system outlet was initially set.

The main outcome of the working limits definition is summarized in Fig. 13 for a comprehensive visualization that gathers all operational boundaries for the given ambient conditions. Such representation allows to visualize how the defined limits interact with the system capacity of providing a certain steam mass flow rate for a certain value of the ambient temperature at the inlet of the GT compressor. More precisely, these are the graphical views of the maps queried by the model at each timestep with the steam demand and ambient temperature values, returning as output the optimal performance of the cogeneration system that complies with all the predefined boundaries. The white area is the area that can be covered by the CHP, while the different limits and their interaction with machine operation are represented by the different colored areas, each corresponding to a different limitation. Building on these results, further consideration has been made accounting for the combustion products and properties of hydrogen, which is the fuel fed to the system. Usually, when referring to conventional power plants, flue gases (also known as stack gases) refer to the gaseous mixture released from the combustion of fossil fuels, consisting of the reaction products, together with residual substances such as particulate matter (dust), sulphur oxides, nitrogen oxides and carbon monoxide and dioxide. The main limitations at the stack are the possibility of acid condensation related to the sulphur content of the fuel and the rising properties of the plume [118]. The higher the temperature at the stack, the more it will be possible to avoid the associated criticalities, which is why a lower output temperature limit is usually set (363 K for this case). As hydrogen replaces hydrocarbons in the fuel composition neither acidic condensate nor CO or CO_2 are present as combustion by-products due to the absence of carbon or sulphur in the combustion reaction [119]. For this reason, it

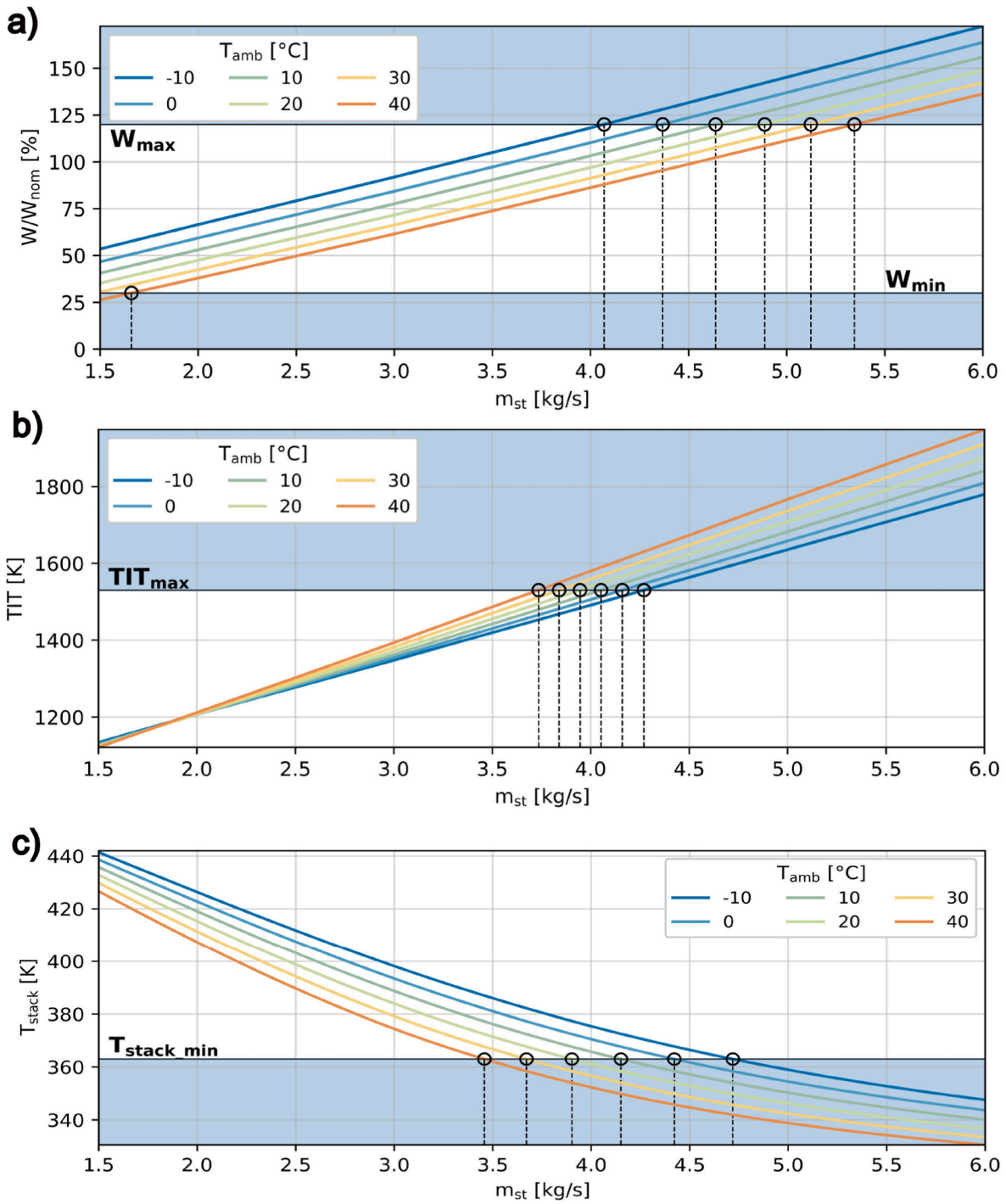

Fig. 12. Operation limits for the cogeneration system varying ambient temperature and steam mass flow rate production: Power load (a), TIT (b), Stack temperature (c).

was decided to no longer consider the stack temperature as an operational limit. This assumption has a beneficial effect on the system potential and resulted in a 2% increase in working hours of the cogeneration unit.

3.1.2. Simulation

After the development and validation of the model, annual simulations were performed for the case study under consideration. Starting from the demand for saturated steam in the paper mill, runs were carried out in a thermal-follow configuration, in order to prioritize meeting the industry thermal load. Main results are reported and discussed below.

Fig. 14 illustrates the hourly steam demand of the facility compared to the cogeneration system production capacity. Both minimum and maximum producibility value is computed for each timestep and represented in the plot as the blue (bottom) and orange (top) line. Scattered dots are spread in a range of (0.38÷5.22) kg/s representing papermill needs that are mostly met by the cogeneration plant (blue area).

The control logic, as presented in Section 2.3, allows for the activation of an additional steam generator when the need exceeds the maximum producibility, while for loads lower than the minimum, the diverter is activated discharging part of the flue gases into the environment. The latter situation occurs only 74 times per year,

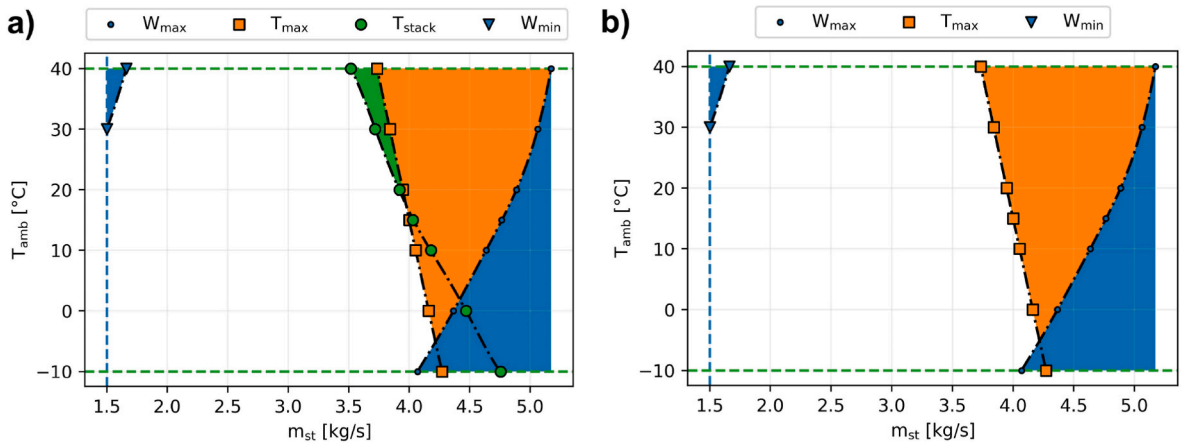

Fig. 13. CHP operational maps visualization for two cases: accounting (a) and neglecting (b) temperature limitations at stack.

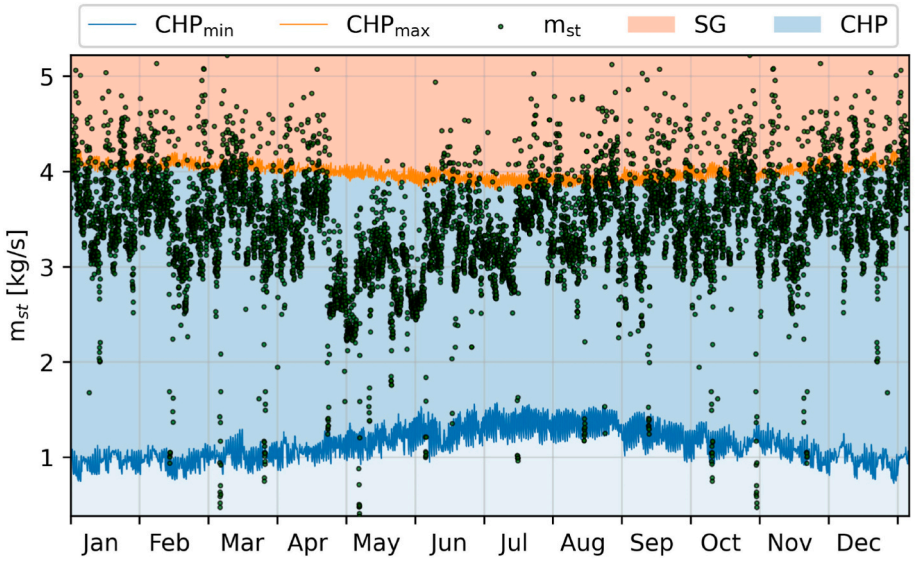

Fig. 14. Annual operations of the cogeneration plant visualizing hourly operational boundaries of the system and facility steam demand.

concentrated in short periods of low demand, confirming that the assumption made about the control logic has a relatively low influence on the results of the analysis, and the cogeneration system is well-sized. As an example, Fig. 15 illustrates the operation of the system during a week in April, comparing the trends of energy demand and production. As shown in Fig. 15 (a), the thermal demand is mainly met by the cogenerator, while for peak production (in red), the auxiliary steam generator is activated. The situation is different for the electrical load, as illustrated in Fig. 15 (b). The turbine generates electricity based on the thermal demand, thus the production and demand curves are not independent. Therefore, situations of overproduction can occur, where excess energy is fed into the grid (blue area), as well as deficits where energy must be purchased from the grid to meet demand (red area).

The overall cogeneration performance results are summarized by the global efficiency indicator, which stands at a high value of 0.86, in line with traditional industrial applications. Furthermore, considering that the fuel used is hydrogen, which is completely carbon-free, it is possible to quantify the actual impact on the decarbonization of the paper mill's consumption. After analyzing the results, it was possible to estimate the savings in terms of CO_2 emissions, which were calculated by referring to the amount of natural gas that would have been burned if the plant had been operated traditionally. From this number, the emissions derived from the consumption of energy purchased from the grid were subtracted, and weighted with respect to the carbon intensity of the Italian electricity grid, presenting an average value of 226 $kgCO_2$/MWh in 2021 [120].

These calculations demonstrate that the CO_2 savings amount to a significant quantity of 29,279 t/y. Analyzing in more detail the performance of the thermal power plant, it can be observed that the CHP can meet the thermal load in terms of duration for 89% of the annual period (with the auxiliary steam generator activated for 982 h/y) and 99% of the thermal demand. The overall thermal efficiency stands at 0.56. As for the electrical part, the efficiency drops to 0.29 and the load coverage is at 92% of the total.

Based on these results, it was possible to derive the hourly consumption of hydrogen fuel required for the desired operation of the cogeneration system. The final result takes into account both the hydrogen fed to the turbine and that consumed in the auxiliary SG, totalling 4,209 t/y. This result is of fundamental importance for the prosecution of the analysis, intended at defining the optimal size for the dedicated green hydrogen production plant among many different possible configurations.

3.2. *Green hydrogen production system*

In order to meet the demand of the facility, all the feasible couplings

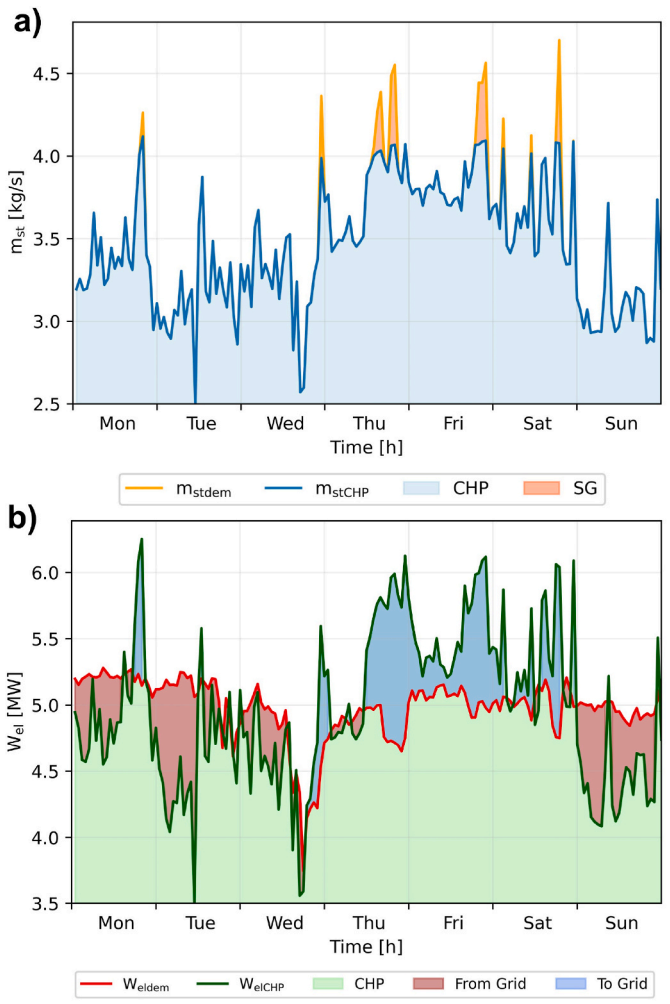

Fig. 15. Weekly operation of CHP system and load interaction: thermal load (a), electricity (b).

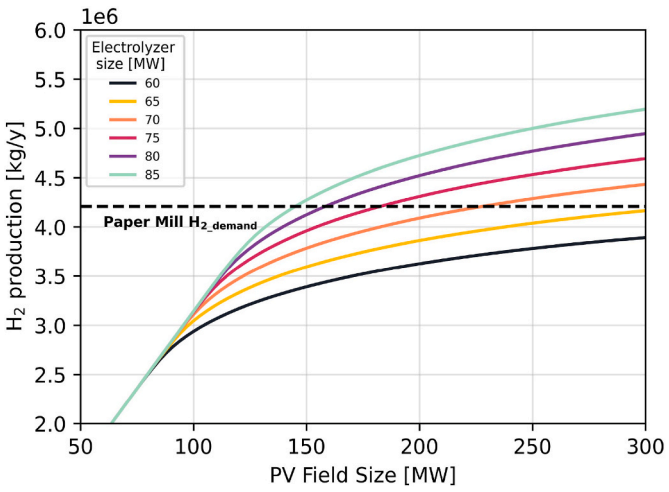

Fig. 16. Hydrogen production comparing different electorlyzer stack sizes coupled with increasing PV field capacities.

in terms of PV farm and electrolyzer size are simulated considering one-year operation with the aim of producing the amount of hydrogen needed to fuel the industry. Many different configurations are evaluated as presented in Section 2.7 and main results from the thermodynamic simulations are presented in Fig. 16. The pairs that satisfy the objective function are those identified by the intersection of the black dashed line with the set of curves produced via the simulation of the energy system, each of them representing a specific electrolyzers capacity, i.e., the pairs ensuring that the plant hydrogen demand is fully satisfied with no excess of production over the span of one year. It can be observed that for each electrolyzer size, as the power of the PV system increases, production saturation is reached, as can be seen by the flattening of the curves.

Among the many different possible outcomes, all feasible solutions lying on the black line in the plot have been defined, resulting in a variation range for the PV farm of (134÷300) MW while the electrolyzer stack is evaluated between (66÷109) MW rated power. In fact, for a PV field size lower than 134 MW, there is not any electrolyzers size capable to produce through the year the total amount of hydrogen requested from the facility. Each of the analyzed configurations can satisfy the annual needs leading to different expenditures, and energy balances.

In Fig. 17 (a) the resulting size combinations of solar and electrolytic systems are plotted in red, alongside the corresponding required hydrogen storage size. The size needed for the storage system is not predetermined, rather it is strictly dependent on the production capacity of the system and the demand of the facility. It is interesting to observe that, starting from a value of 134 MW of installed solar capacity and 109 MW of electrolyzers, the corresponding storage size is 756 t, while increasing the size of the photovoltaic plant, there is a decrease in both the required electrolytic capacity and the size of the storage tanks, to values that for a 300 MW photovoltaic field are 66 MW and 656 t of hydrogen, respectively. It can therefore be derived that as the availability of renewable resources increases, a greater exploitation of the installed electrolytic potential is achieved, improving the capacity factor of the fleet, which therefore needs fewer units to be kept operational for longer. As a consequence, the storage capacity decreases accordingly, as more hydrogen is produced and simultaneously consumed by the CHP. Since the identified couplings are all feasible from a thermodynamic point of view, the one defined as optimal is found through a detailed economic analysis. Thus, several major economic key performance indicators are evaluated for each of the feasible combinations. Fig. 17 (b) displays the results obtained for the profit index and the payback time calculated over an investment lifetime of 20 years; all the major economic assumptions are presented in Section 2.8.

The optimal configuration was then defined by seeking the maximum value on the PI curve and the minimum payback time, which in this case coincide, being 0.35 for the former and 12.4 years for the latter parameter, corresponding to a PV field of 244 MW and an electrolyzer stack of 69 MW of rated power. Depending on the defined hydrogen production plant size, a storage system with a capacity of 677 t is required. The trend of the state of charge of the tank system is depicted in Fig. 18 and gives an overview of how seasonality affects production from renewables and hence the hydrogen storage evolution over time. During the summer months, there is a notable rise in production that surpasses the trend for hydrogen demand, the PV production peak corresponds to minimum demand over the year, therefore resulting in a steep increase in the tank state of charge before the winter season. Stored hydrogen is then consumed at a higher rate when solar resource is scarce. It is important to note how the need for a storage system of such large dimensions is due, in addition to the relatively low pressure considered (30 bar), to the mismatch between the production capacity of renewable sources, which are concentrated exclusively during daylight hours, and the demand for fuel in a continuous process such as paper manufacturing, which has high and constant rates of energy consumption 24 h per day.

Having defined the storage tanks size, it is important to provide further considerations addressing the insights, limitations, and feasibility of the proposed solution. The primary goal of the analysis was to define how much hydrogen would need to be stored in order to meet both the problem boundary conditions and the defined objective function. Although main findings are linked to the hourly hydrogen mass

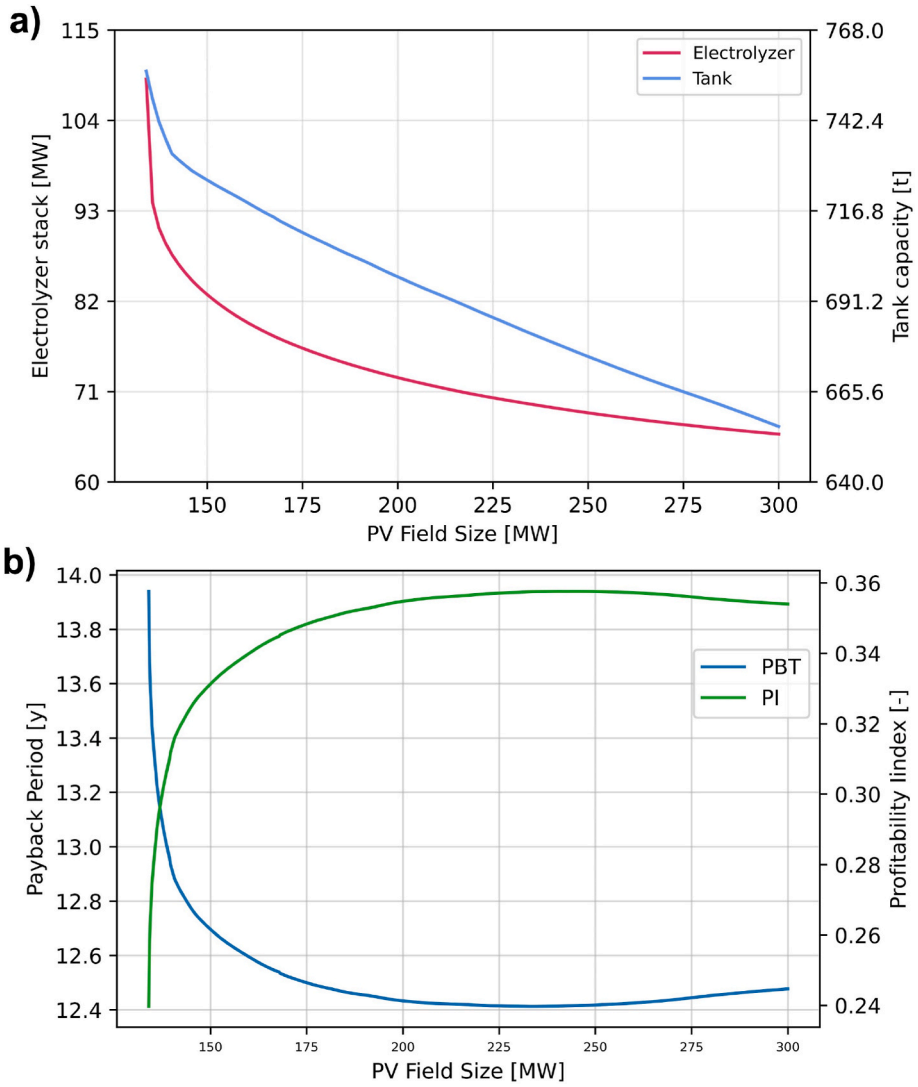

Fig. 17. Different capacity pairs of solar fields and electrolyzers satisfying papermill hydrogen demand. System dimensions (a), economic analysis (b).

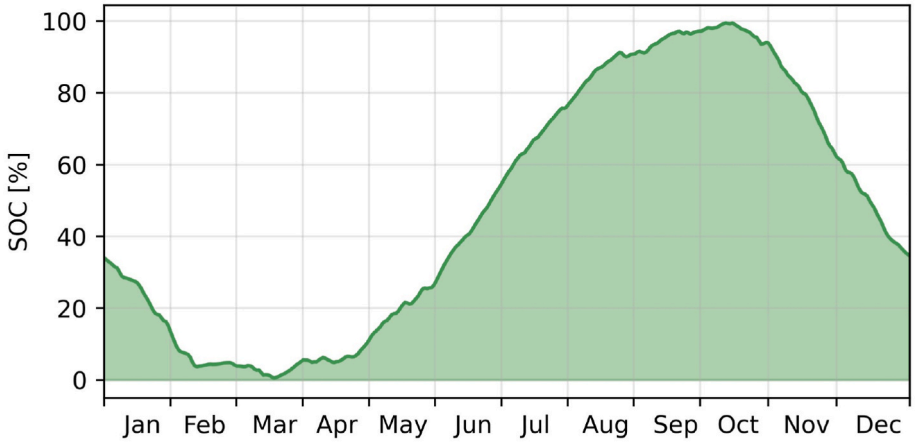

Fig. 18. Hydrogen storage tank system level of charge during the year.

flow rate, in addressing feasibility issues, the pressure considered for the storage would result in the prohibitive volumetric footprint of 0.4 m^3/kg, which is hardly suitable for industrial-sized application.

As a mean of comparison, under simple assumptions, considering a specific consumption of 2.021 kWh/kg for a compressor to take hydrogen from the outlet level of the electrolyzer to 300 bar [121], would reduce the storage volumetric footprint of 88% (0.047 m^3/kg) by requiring only 3.6% of the electricity consumed by the electrolyzers

stack and just 1.33% of the capital cost expenditures of the hydrogen production chain components. Cost have been calculated considering maximum throughput of the compression system (0.34 kg/s) as indicated in the cost correlation presented by Mayer et al. [122]. It is therefore evident that hydrogen storage at 300 bar offers a potential solution to overcome the space limitations associated with storing hydrogen at the electrolyzer outlet level, with minimal energy and economic implications. However, it should be noted that, according to the results presented in Moran et al. [123], underground storage emerges as the potentially optimal solution to handle the quantities considered in large-scale applications. It is nonetheless important to highlight that its main limitations persist in the form of geographical scarcity, necessity for hydrogen purification at the cavern outlet and the fact that this concept has not yet been confirmed on an industrial-scale [124]. Accordingly to the forgoing considerations, for the purpose of this study, technical feasibility of low-pressure storage has not been addressed in detail.

In terms of economic results of the optimal configuration, despite representing the maximum achievable value, a PI of 0.35 indicates a relatively low profitability and can be justified only by considering the high capital expenditures due to the large size of the hydrogen production and storage plant required. However, it is important to note that this PI value is matched by a positive NPV, suggesting that the investment generates a positive return over its lifetime. With the chosen configuration, the total electricity to be purchased from the grid during the year is equal to 2 GWh assessing the good performance of the CHP plant, while the total electricity surplus to be fed back into the grid is equal to 193 GWh. This demonstrates how high is the impact of a strongly volatile energy source as the solar one. As a consequence, the total required initial investment is equal to 60 M€ for each MW of the CHP plant (for a total of 363 M€) and 99% of these are due to the H_2 supply chain component capital costs (54% to the tank, 35% to the PV field and 10% to the electrolyzers). Delving into the economic evaluation in more detail, it was possible to calculate the LCOH value for the chosen configuration, which was found to be 6.41 €/kg, placing it in the lowest cost range among those reproduced in similar studies related to the sector where a value ranging in the (4÷13) €/kg interval is presented [60]. Although this value remains considerably higher than the current market price of 'grey' hydrogen, which fluctuates between 1 €/kg and 2 €/kg [125], it is nevertheless a good indicator of the feasibility of similar investments in the decarbonization process of heavy industries, especially considering the decreasing cost trend of hydrogen technologies. Irena [126] suggests that the cost of hydrogen electrolyzers could decrease over the next decade at rates similar to those recorded for solar panels and wind turbines, by 82% and 39% respectively between 2010 and 2019. Similarly, research into new materials and the growing demand for hydrogen tanks could lead to similar price reductions for these components. As the initial investment costs decrease, due also to incentives derived from new energy policies, and taking into account the rising costs of fossil energy sources, a 6.41 €/kg value constitutes a good starting point for the market competitiveness of these systems compared to non-renewable methods of hydrogen production.

Further considerations can be drawn by weighing the contribution of each of the technologies used on the final hydrogen cost. It has to be emphasized that this calculation only takes into account the energy and economic components and flows involved in the hydrogen production system, and not those related to its final utilization, although they are considered within the scope of the broader analysis. This visualization provides a better understanding of how the assumptions made in terms of plant and control logic influence the sizing and thus the unit cost of renewable hydrogen. Analysing the pie chart presented in Fig. 19, it can be observed how great is the influence of the storage system on the total balance, accounting for more than half of the total cost (57.2%). On the other hand, the PV field and electrolyzers respectively influence one-sixth and one-eighth of the cost of hydrogen, with the remaining contribution coming from the operation and maintenance costs, which

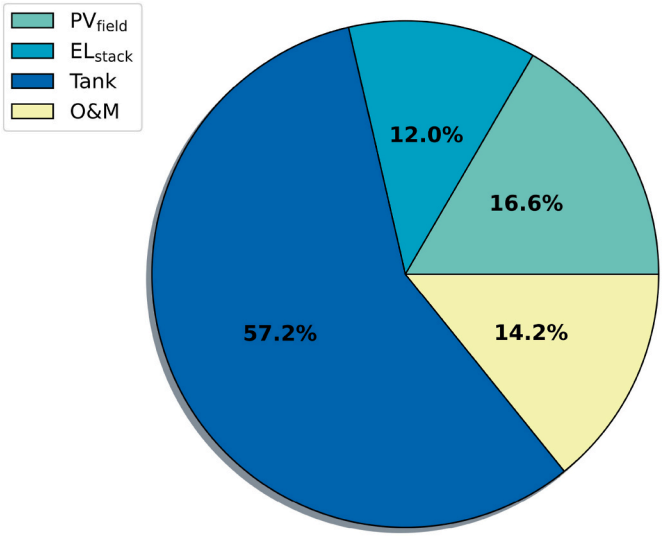

Fig. 19. Representation of the different contributions to the formation of the final LCOH value.

are the third largest cost element for a system of this size.

From these results, it can be inferred that the assumption of producing on-site renewable hydrogen for PtP applications through the sole contribution of a dedicated plant without considering the interaction with the grid or other sources of supply leads to the need for a huge storage system.

In this case, more suitable alternative solutions could be increasing the storage pressure up to liquefaction or implementing an underground storage system if the geological characterization of the site allows it. After that, the LCOE for the chosen configuration has been assessed and it was found to be equal to 14.05 c€/kWh. This cost has been calculated without considering any differences between the electricity surplus generated by the PV field and the electricity produced by the CHP plant, even if the latter has obviously a higher value. Though, in order to assess the performance of a system like this, the best parameter to be presented is the LCOH and not the LCOE.

Finally, a sensitivity analysis was carried out on the NPV of the optimal plant to evaluate its performance in comparison with the baseline scenario of traditional natural gas CHP system operation accounting for the variation in fossil fuel purchase price. The impact of this variation has a tangible effect on the NPV trend, making it a fundamental factor in achieving the investment payback at the end of its life, as represented in Fig. 20.

The natural gas price is considered in the analysis as a positive cash flow in terms of savings compared to the traditional configuration. In this case, the cogeneration plant under investigation would consume 10,644 10 t/y of natural gas, which, however, if replaced 100% by green hydrogen, would result in significant savings both in terms of cost and environmental impact.

Therefore, financing through the ETS system was also taken into account, which guarantees funding of 86.6 €/t for every ton of direct CO_2 emissions avoided. The high fluctuation of gas prices is an extremely important factor in the economy of energy-intensive sectors such as the paper industry. Therefore, the fluctuating trend observed over the past year due to the complex international geopolitical situation is an element to pay close attention to when planning current and future efforts in decarbonizing industry. Given the significant fluctuations exhibited by Dutch TTF Futures in 2022, which peaked at 340 €/MWh in late August before declining to 120 €/MWh in December [127], a variation range of 80 €/MWh to 360 €/MWh was selected to be as representative as possible of the highly volatile energy scenarios. All curves exhibit an increasing trend, meaning that positive cash flows due

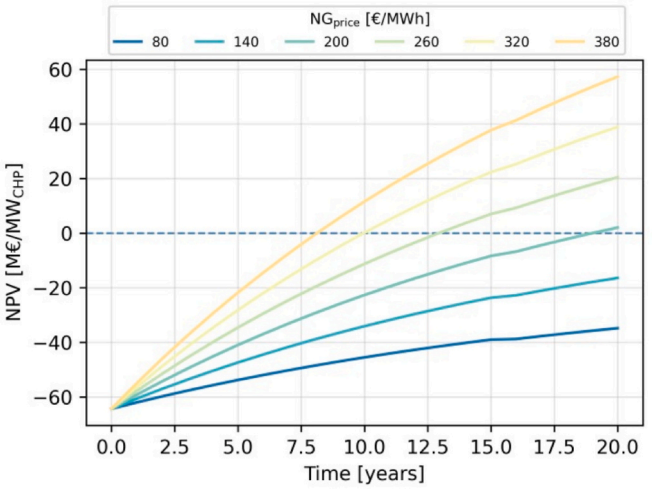

Fig. 20. Sensibility analysis on NPV of the optimal plant configuration varying natural gas price.

to the sum of savings and revenues derived from the decarbonization intervention, exceed the operational costs for the system. A slight discontinuity can be observed in each of the curves, which is attributed to the replacement of the electrolysis system requiring intervention after 15 years of operation. It turns out that low gas prices do not allow for a return on investment, or only permit it at the end of the asset lifespan. On the other hand, payback periods of less than 10 years are only observed for costs exceeding 260 €/MWh.

Results have therefore shown that the economic feasibility of decarbonizing the paper industry through such interventions is strongly dependent on the prices of traditional fuel. This certainly highlights the need for individual states to increase their energy security and free themselves from dependence on entities subject to unpredictable geopolitical dynamics. Moreover, the significant investment required to enable the adoption of green hydrogen in such systems is the most significant sign of the need for specific incentive policies that can reduce prohibitive costs and enable rapid and widespread adoption of similar solutions in the heavy industry sector. This uptake has also a beneficial side-effect which is the potential to trigger a positive impact on the cost trend of hydrogen production, storage and consumption technologies, expected to decrease as their rate of adoption increases.

4. Conclusions

In this study, a techno-economic feasibility analysis was presented for the decarbonization of paper industry consumption through the use of hydrogen as a vector. The holistic assessment proposed is based on the assumption of the conversion of an existing cogeneration plant based on 100% hydrogen-fuelled gas turbine technology with green hydrogen produced locally through solar energy. The work was divided into two main and consequential strands. Given the consumption of the paper mill under analysis and considering the most recent industrial initiatives to innovate PtX systems, it was possible to size the optimal dedicated cogeneration system starting with minimal plant modifications compared to the traditional natural gas configuration The hydrogen operation of the plant was then addressed in detail, establishing the limits and potential of the system in meeting the annual energy demand according to the thermal-load follow configuration, dependent on environmental conditions. Operational maps were modelled by considering the system running on 100% green hydrogen, thus defining the behavior and consequent limitations posed by the main thermodynamic parameters of the cogeneration plant. From this analysis, the exact hydrogen consumption of the cogeneration system was derived, and the optimal dimensioning of the dedicated multi-energy system for hydrogen production through solar energy was then carried out according to an operational logic that prioritizes it over other energy flows. Results showed that with minimal technological modifications and low costs, a conventional cogeneration plant can be retrofitted to run on sustainable fuel, guaranteeing high performance. By analyzing the operational maps of the CHP system that define the behavior of the main thermodynamic parameters and take into account the TIT and electrical load limits, but allow for the neglection of the minimum temperature limit at the stack, an overall plant efficiency of 0.86 was measured for the considered operating period. This value is in line with the performance of traditional systems and represents an important technical result that highlights the suitability of these systems in industrial contexts, with comparable performance. In addition, significant added value derives from the complete decarbonization of consumption which, accounting for a consumption of green hydrogen of approximately 4,209 t/y, allows a saving of 29,273 t/y of direct CO_2 emissions into the atmosphere that can be economically valorized according to the ETS scheme.

After incorporating the results produced by the simulation of the cogeneration system, the study proceeded with the simulation and sizing of dedicated production and storage systems following a simulation-based parametric approach. Among the many possible configurations satisfying the constraints set in the study, the one with the best possible economic outcome was chosen, based on an IP of 0.35 and an estimated return on investment of 12.4 years. The value obtained for LOCH is 6.41 €/kg which is still far from being competitive with the cost of grey and blue hydrogen but nonetheless in the lower range of literature values. This is also associated with an LCOE value of 14.05 c€/kWh, which compares well with several similar studies in the literature. In light of these considerations, the presented methodology and results provide insights that can serve as a foundation for future research. Specifically, the findings of this study can be considered as a benchmark for further investigations aimed at developing more sophisticated optimization algorithms to address similar problems in the decarbonization of industry.

PtX systems of this size are still prohibitively expensive and unprofitable in terms of investment unless supported by specific incentive policies that promote their adoption in industrial settings. Therefore, the results generated are bound to guide more in-depth studies that should evaluate different configurations and business models, such as the effect of considering different renewable sources, electrical storage solutions or the interaction with the grid and the related repercussions on the electrolysis system, also exploring the possibility of evaluating operation based on the cost of electricity or the present value of the carbon intensity of the grid. The adoption of several innovative hydrogen-related cogeneration technologies also deserves further investigation, such as solid oxide fuel cells that can simultaneously produce electricity and heat. Furthermore, social and environmental analyses should be considered as necessary assessments to understand the overall feasibility of such systems.

Building on the results presented in this study, it is important to understand how to further reduce the cost of these systems by taking advantage of various synergies, such as the exploitation of existing infrastructure and/or by-products of the hydrogen production or consumption process. Finally, future work should also consider the introduction of uncertainty quantification methods to estimate how different assumptions may affect the results obtained, taking into account factors such as weather variability, different electricity prices and technology cost projections.

Declaration of competing interest

The authors declare that they have no known competing financial interests or personal relationships that could have appeared to influence the work reported in this paper.

Data availability

Data will be made available on request.

Acknowledgements

This research did not receive any specific grant from funding agencies in the public, commercial, or not-for-profit sectors.

Nomenclature

Symbols

CRF	Capital Recovery Factor [−]
E_{cell}	Open circuit potential [V]
ξ	PV utilization factor [−]
i	Current density [A/cm^2]
I_0	Total investment [€]
L_{act}	Activation overpotential [V]
L_{conc}	Concentration overpotential [V]
L_{ohm}	Ohmic overpotential [V]
m	Mass flow rate [kg/s]
N	Investment years [years]
N_{cell}	Number of cells [−]
p	Pressure [Pa]
r	Weighted average cost of capital [−]
SF	Scale Factor [−]
T	Temperature [K]
V_{stack}	Stack potential [V]
W	Power [MW]
η	Efficiency [−]

Subscripts

amb	Ambient
app	Approach
CO_2	Carbon Dioxide
dem	Demand
des	Design
el	Electrical
ele	Electrolyzer
exh	exhaust
fuel	Hydrogen fuel
GT	Gas Turbine
H_2	Hydrogen
H_2O	Water
Nom	Nominal
O_2	Oxygen
pp	Pinch point
price	Price
prod	Produced
ref	reference
rep	Replacement
size	Size
sat	Saturation
st	Steam
sub	Sub-cooling
tank	Tank
tech	Technology
tot	Total
unit	Unit
wa	Working Area

Acronyms

AEL	Alkaline Electrolyzer
CAPEX	Capital Expenditure
CF	Cash Flow
CHP	Combined Heat and Power
ESMS	Energy System Modular Solver
ETS	Emissions Trading System

GT	Gas Turbine
HRSG	Heat Recovery Steam Generator
ISO	International Organization for Standardization
LCOE	Levelized Cost of Electricity
LCOH	Levelized Cost Of Hydrogen
MR	Maximum Rectangle
NG	Natural Gas
NPV	Net Present Value
O&M	Operation & Maintenance
OPEX	Operational Expenditure
PI	Profitability Index
PBP	Payback Period
PEMEL	Polymer Exchange Membrane Electorlyzer
PV	Photovoltaic
PtG	Power to Gas
PtX	Power to X
PtP	Power to Power
RES	Renewable Energy Sources
REV	Revenues
SOC	State Of Charge
SOEL	Solide Oxide Electorlyzer
SG	Steam Generator
ST	Stack Temperature
TIT	Turbine Inlet Temperature

References

[1] Arias P, Bellouin N, Coppola E, Jones R, Krinner G, Marotzke J, et al. Climate change 2021: the physical science basis. Contribution of working group I to the sixth assessment report of the intergovernmental panel on climate change; technical summary. In: Masson-Delmotte V, Zhai P, Pirani A, Conners SL, Péan C, Berger S, et al., editors. Intergov. Panel clim. Chang. AR6; 2021.

[2] Schleussner C-F, Rogelj J, Schaeffer M, Lissner T, Licker R, Fischer EM, et al. Science and policy characteristics of the Paris Agreement temperature goal. Nat Clim Change 2016;6:827–35. https://doi.org/10.1038/nclimate3096.

[3] European Commission (EC). The European Green Deal n.d. https://eur-lex.europa.eu/legal-content/EN/TXT/?uri=COM%3A2019%3A640%3AFIN. [Accessed 17 October 2022].

[4] EU. Directive (EU) 2018/2001 of the European Parliament and of the Council on the promotion of the use of energy from renewable sources. Off J Eur Union 2018;2018:82–209.

[5] Industry – Analysis - IEA n.d. https://www.iea.org/reports/industry. [Accessed 11 January 2023].

[6] Net zero emissions by 2050 scenario (NZE) – global energy and climate model – analysis - IEA n.d. https://www.iea.org/reports/global-energy-and-climate-model/net-zero-emissions-by-2050-scenario-nze. [Accessed 11 January 2023].

[7] Pulp and paper – analysis - IEA n.d. https://www.iea.org/reports/pulp-and-paper. [Accessed 11 January 2023].

[8] Pulp and paper industry — global efficiency intelligence n.d. https://www.globalefficiencyintel.com/pulp-and-paper-industry. [Accessed 11 January 2023].

[9] Szabó L, Soria A, Forsström J, Keränen JT, Hytönen E. A world model of the pulp and paper industry: demand, energy consumption and emission scenarios to 2030. Environ Sci Pol 2009;12:257–69. https://doi.org/10.1016/J.ENVSCI.2009.01.011.

[10] Boyce MP. Handbook for cogeneration and combined cycle power plants. second ed. New York, NY: The American Society of Mechanical Engineers; 2010.

[11] Bhander G, Jozewicz W. Energy and Emission Control Technologies Dovepress Analysis of emission reduction strategies for power boilers in the US pulp and paper industry. https://doi.org/10.2147/EECT.S139648; 2017.

[12] Monte MC, Fuente E, Blanco A, Negro C. Waste management from pulp and paper production in the European Union. Waste Manag 2009;29:293–308. https://doi.org/10.1016/J.WASMAN.2008.02.002.

[13] Holmberg H, Tuomaala M, Haikonen T, Ahtila P. Allocation of fuel costs and CO2-emissions to heat and power in an industrial CHP plant: case integrated pulp and paper mill. Appl Energy 2012;93:614–23. https://doi.org/10.1016/J.APENERGY.2011.11.040.

[14] Möllersten K, Gao L, Yan J, Obersteiner M. Efficient energy systems with CO2 capture and storage from renewable biomass in pulp and paper mills. Renew Energy 2004;29:1583–98. https://doi.org/10.1016/J.RENENE.2004.01.003.

[15] Shabbir I, Mirzaeian M. Feasibility analysis of different cogeneration systems for a paper mill to improve its energy efficiency. Int J Hydrogen Energy 2016;41:16535–48. https://doi.org/10.1016/J.IJHYDENE.2016.05.215.

[16] Acar C, Dincer I. Comparative assessment of hydrogen production methods from renewable and non-renewable sources. Int J Hydrogen Energy 2014;39:1–12. https://doi.org/10.1016/J.IJHYDENE.2013.10.060.

[17] Garcia DA, Barbanera F, Cumo F, Di Matteo U, Nastasi B. Expert opinion analysis on renewable hydrogen storage systems potential in Europe. Energies 2016;9. https://doi.org/10.3390/en9110963.

[18] Guandalini G, Campanari S, Romano MC. Power-to-gas plants and gas turbines for improved wind energy dispatchability: energy and economic assessment. Appl Energy 2015;147:117–30. https://doi.org/10.1016/J.APENERGY.2015.02.055.

[19] Griffin PW, Hammond GP, Norman JB. Industrial decarbonisation of the pulp and paper sector: a UK perspective. Appl Therm Eng 2018;134:152–62. https://doi.org/10.1016/J.APPLTHERMALENG.2018.01.126.

[20] Sun M, Wang Y, Shi L, Klemeš JJ. Uncovering energy use, carbon emissions and environmental burdens of pulp and paper industry: a systematic review and meta-analysis. Renew Sustain Energy Rev 2018;92:823–33. https://doi.org/10.1016/J.RSER.2018.04.036.

[21] Kong L, Hasanbeigi A, Price L. Assessment of emerging energy-efficiency technologies for the pulp and paper industry: a technical review. J Clean Prod 2016;122:5–28. https://doi.org/10.1016/J.JCLEPRO.2015.12.116.

[22] Marshman DJ, Chmelyk T, Sidhu MS, Gopaluni RB, Dumont GA. Energy optimization in a pulp and paper mill cogeneration facility. Appl Energy 2010;87:3514–25. https://doi.org/10.1016/J.APENERGY.2010.04.023.

[23] Ahmadi P, Almasi A, Shahriyari M, Dincer I. Multi-objective optimization of a combined heat and power (CHP) system for heating purpose in a paper mill using evolutionary algorithm. Int J Energy Res 2012;36:46–63. https://doi.org/10.1002/ER.1781.

[24] Gambini M, Vellini M, Stilo T, Manno M, Bellocchi S. High-efficiency cogeneration systems: the case of the paper industry in Italy. Energies 2019;12. https://doi.org/10.3390/en12030335.

[25] Yamaki A, Fujii S, Kanematsu Y, Kikuchi Y. Life cycle greenhouse gas emissions of cogeneration energy hubs at Japanese paper mills with thermal energy storage. Energy 2023:270. https://doi.org/10.1016/J.ENERGY.2023.126886.

[26] Najjar YSH. Gas turbine cogeneration systems: a review of some novel cycles. Appl Therm Eng 2000;20:179–97. https://doi.org/10.1016/S1359-4311(99)00019-8.

[27] Poullikkas A. An overview of current and future sustainable gas turbine technologies. Renew Sustain Energy Rev 2005;9:409–43. https://doi.org/10.1016/J.RSER.2004.05.009.

[28] Nadir M, Ghenaiet A, Carcasci C. Thermo-economic optimization of heat recovery steam generator for a range of gas turbine exhaust temperatures. Appl Therm Eng 2016;106:811–26. https://doi.org/10.1016/J.APPLTHERMALENG.2016.06.035.

[29] Desideri U, Garroni E, Proietti S. Repowering of a gas turbine based CHP in a pulp and paper industry. 2009. p. 693–702. https://doi.org/10.1115/GT2009-60233.

[30] Naqvi M, Yan J, Dahlquist E. Black liquor gasification integrated in pulp and paper mills: a critical review. Bioresour Technol 2010;101:8001–15. https://doi.org/10.1016/J.BIORTECH.2010.05.013.

[31] Dodds PE, Staffell I, Hawkes AD, Li F, Grünewald P, McDowall W, et al. Hydrogen and fuel cell technologies for heating: a review. Int J Hydrogen Energy 2015;40:2065–83. https://doi.org/10.1016/J.IJHYDENE.2014.11.059.

[32] Skordoulias N, Koytsoumpa I, Karellas S. Techno-economic evaluation of medium scale power to hydrogen to combined heat and power generation systems. https://doi.org/10.1016/j.ijhydene.2022.06.057; 2022.

[33] Lund H, Østergaard PA, Connolly D, Mathiesen BV. Smart energy and smart energy systems. Energy 2017;137:556–65. https://doi.org/10.1016/J.ENERGY.2017.05.123.

[34] Mathiesen BV, Lund H, Connolly D, Wenzel H, Østergaard PA, Möller B, et al. Smart Energy Systems for coherent 100% renewable energy and transport solutions. https://doi.org/10.1016/j.apenergy.2015.01.075; 2015.
[35] Ridjan I, Mathiesen BV, Connolly D. Synthetic fuel production costs by means of solid oxide electrolysis cells. Energy 2014;76:104–13. https://doi.org/10.1016/J.ENERGY.2014.04.002.
[36] Rahman MN, Wahid MA. Renewable-based zero-carbon fuels for the use of power generation: a case study in Malaysia supported by updated developments worldwide. Energy Rep 2021;7:1986–2020. https://doi.org/10.1016/J.EGYR.2021.04.005.
[37] van Wijk A, Chatzimarkakis J. Green hydrogen for a European green deal a 2x40 GW initiative. Hydrog Eur 2020:41. –p.
[38] Superchi F, Mati A, Pasqui M, Carcasci C, Bianchini A. Techno-economic study on green hydrogen production and use in hard-to-abate industrial sectors. J Phys Conf Ser 2022. https://doi.org/10.1088/1742-6596/2385/1/012054.
[39] Johannsen RM, Mathiesen BV, Kermeli K, Crijns-Graus W, Østergaard PA. Exploring pathways to 100% renewable energy in European industry. Energy 2023;268:126687. https://doi.org/10.1016/J.ENERGY.2023.126687.
[40] Kosturjak A, Dey T, Young M, Whetton S. Advancing Hydrogen: learning from 19 plans to advance hydrogen from across the globe. 2019. p. 1–121.
[41] Burton NA, Padilla RV, Rose A, Habibullah H. Increasing the efficiency of hydrogen production from solar powered water electrolysis. Renew Sustain Energy Rev 2021;135. https://doi.org/10.1016/J.RSER.2020.110255.
[42] Pandey AP, Bhatnagar A, Shukla V, Soni PK, Singh S, Verma SK, et al. Hydrogen storage properties of carbon aerogel synthesized by ambient pressure drying using new catalyst triethylamine. Int J Hydrogen Energy 2020;45:30818–27. https://doi.org/10.1016/J.IJHYDENE.2020.08.145.
[43] Siemens and Uniper join forces to decarbonize power generation | Uniper n.d. https://www.uniper.energy/sustainability/sustainability-resources/siemens-and-uniper-join-forces-decarbonize-power-generation. [Accessed 25 February 2023].
[44] Witzel B, Moëll D, Parsania N, Yilmaz E, Koenig M. Development of a fuel flexible H2-natural gas gas turbine combustion technology platform. Proc ASME Turbo Expo 2022;3-B. https://doi.org/10.1115/GT2022-82881.
[45] INIS repository search - single result. n.d, https://inis.iaea.org/search/searchsinglerecord.aspx?recordsFor=SingleRecord&RN=51108041. [Accessed 16 January 2023].
[46] Hyflexpower completes power-to-hydrogen-to-power in France. n.d, https://www.industryandenergy.eu/hydrogen/hyflexpower-completes-power-to-hydrogen-to-power-in-france/. [Accessed 16 January 2023].
[47] Prasad VN. Hydrogen as a path to sector-coupled deep decarbonization. Soc pet eng - Abu Dhabi int pet exhib conf 2020. ADIP 2020; 2020. https://doi.org/10.2118/202999-MS.
[48] HYdrogen as a FLEXible energy storage for a fully renewable European POWER system | HYFLEXPOWER Project | Fact Sheet | H2020 | CORDIS | European Commission n.d. https://cordis.europa.eu/project/id/884229 (accessed January 16, 2023).
[49] About - hyflexpower. n.d. . [Accessed 16 January 2023]. http://www.hyflexpower.eu/about/?_gl=1*1bhb6ci*_ga*OTg3Mzk5NDkyLjE2NzM4NzIxODk.*_up*MQ
[50] Escamilla A, Sánchez D, García-Rodríguez L. Assessment of power-to-power renewable energy storage based on the smart integration of hydrogen and micro gas turbine technologies. Int J Hydrogen Energy 2022;47:17505–25. https://doi.org/10.1016/J.IJHYDENE.2022.03.238.
[51] Mitsubishi Power Americas, Inc.. World's largest renewable energy storage project announced in Utah. n.d. https://power.mhi.com/regions/amer/news/190530.html?utm_source=amerweb& utm_medium=release& utm_campaign=DOE. [Accessed 25 February 2023].
[52] Robinson - Robinson nd. https://www.robinson-h2020.eu/. [Accessed 25 February 2023].
[53] FLEXnCONFU – FLEXibilize combined cycle power plant through Power- to-X solutions using CONventional fuels. n.d. https://flexnconfu.eu/. [Accessed 25 February 2023].
[54] HYdrogen as a FLEXible energy storage for a fully renewable European POWER system | HYFLEXPOWER Project | Fact Sheet | H2020 | CORDIS | European Commission n.d. https://cordis.europa.eu/project/id/884229 (accessed February 25, 2023).
[55] Gas turbines in the US are being prepped for a hydrogen-fuelled future. n.d. https://www.nsenergybusiness.com/features/gas-turbines-hydrogen-us/. [Accessed 25 February 2023].
[56] Mitsubishi Power launches green hydrogen "standard package" projects. n.d. https://www.powerengineeringint.com/hydrogen/mitsubishi-power-launches-green-hydrogen-standard-package-projects/. [Accessed 25 February 2023].
[57] Green hysland - deployment of a H2 ecosystem on the Island of Mallorca. n.d. https://greenhysland.eu/. [Accessed 25 February 2023].
[58] Heymann F, Rüdisüli M, vom Scheidt F, Camanho AS. Performance benchmarking of power-to-gas plants using Composite Indicators. Int J Hydrogen Energy 2022;47:24465–80. https://doi.org/10.1016/J.IJHYDENE.2021.10.189.
[59] Crespi E, Colbertaldo P, Guandalini G, Campanari S. Design of hybrid power-to-power systems for continuous clean PV-based energy supply. Int J Hydrogen Energy 2021;46:13691–708. https://doi.org/10.1016/J.IJHYDENE.2020.09.152.
[60] Loisel R, Baranger L, Chemouri N, Spinu S, Pardo S. Economic evaluation of hybrid off-shore wind power and hydrogen storage system. Int J Hydrogen Energy 2015;40:6727–39. https://doi.org/10.1016/J.IJHYDENE.2015.03.117.
[61] Bexten T, Sieker T, Wirsum M. Techno-economic analysis of a hydrogen production and storage system for the on-site fuel supply of hydrogen-fired gas turbines. J Eng Gas Turbines Power 2021;143. https://doi.org/10.1115/1.4052023.
[62] Liponi A, Frate GF, Baccioli A, Ferrari L, Desideri U. Green hydrogen from wind energy: mitigation of operating point fluctuations. In: ECOS 2021-34th int. Conf. Efficency, cost, optim. Simul. Environ. Impact energy syst. ECOS 2021 Program Organizer; 2021. p. 1751–62.
[63] Yue M, Lambert H, Pahon E, Roche R, Jemei S, Hissel D. Hydrogen energy systems: a critical review of technologies, applications, trends and challenges. Renew Sustain Energy Rev 2021;146. https://doi.org/10.1016/J.RSER.2021.111180.
[64] Schmidt O, Gambhir A, Staffell I, Hawkes A, Nelson J, Few S. Future cost and performance of water electrolysis: an expert elicitation study. Int J Hydrogen Energy 2017;42:30470–92. https://doi.org/10.1016/J.IJHYDENE.2017.10.045.
[65] Shiva Kumar S, Himabindu V. Hydrogen production by PEM water electrolysis – a review. Mater Sci Energy Technol 2019;2:442–54. https://doi.org/10.1016/J.MSET.2019.03.002.
[66] Van Der Roest E, Bol R, Fens T, Van Wijk A. Utilisation of waste heat from PEM electrolysers e Unlocking local optimisation. https://doi.org/10.1016/j.ijhydene.2023.03.374; 2023.
[67] Saxe M, Alvfors P. Advantages of integration with industry for electrolytic hydrogen production. Energy 2007;32:42–50. https://doi.org/10.1016/J.ENERGY.2006.01.021.
[68] Refhyne – clean refinery hydrogen for Europe. n.d, https://www.refhyne.eu/. [Accessed 7 February 2023].
[69] H2FUTURE project - startseite. n.d, https://www.h2future-project.eu/. [Accessed 7 February 2023].
[70] Atura Power selects Cummins to design, manufacture 20 MW electrolyzer system for Niagara Hydrogen Centre | Cummins Inc. n.d. https://www.cummins.com/news/releases/2022/10/06/atura-power-selects-cummins-design-manufacture-20-mw-electrolyzer-system (accessed February 7, 2023).
[71] Thomassen MS, Reksten AH, Barnett AO, Khoza T, Ayers K. PEM water electrolysis. Electrochem Power Sources Fundam Syst Appl 2022:199–228. https://doi.org/10.1016/b978-0-12-819424-9.00013-6.
[72] Usman MR. Hydrogen storage methods: review and current status. Renew Sustain Energy Rev 2022;167:112743. https://doi.org/10.1016/J.RSER.2022.112743.
[73] Abe JO, Popoola API, Ajenifuja E, Popoola OM. Hydrogen energy, economy and storage: review and recommendation. Int J Hydrogen Energy 2019;44:15072–86. https://doi.org/10.1016/J.IJHYDENE.2019.04.068.
[74] Yu D, Meng Y, Yan G, Mu G, Li D, Le Blond S. Sizing combined heat and power units and domestic building energy cost optimisation. Energies 2017;10. https://doi.org/10.3390/en10060771.
[75] Shaneb OA, Coates G, Taylor PC. Sizing of residential μcHP systems. Energy Build 2011;43:1991–2001. https://doi.org/10.1016/J.ENBUILD.2011.04.005.
[76] Cardona E, Piacentino A. A validation methodology for a combined heating cooling and power (CHCP) pilot plant. https://doi.org/10.1115/1.1803849; 2004.
[77] Pfenninger S, Staffell I. Long-term patterns of European PV output using 30 years of validated hourly reanalysis and satellite data. Energy 2016;114:1251–65. https://doi.org/10.1016/J.ENERGY.2016.08.060.
[78] Eriksen VL. Heat recovery steam generator technology. Woodhead Publishing; 2017. https://doi.org/10.1115/1.859537.ch7.
[79] SGT-100 | Industrial Gas Turbine | Gas Turbines | Manufacturer | Siemens Energy Global n.d. https://www.siemens-energy.com/global/en/offerings/power-generation/gas-turbines/sgt-100.html (accessed January 17, 2023).
[80] Carcasci C, Facchini B. A numerical method for power plant simulations. Am Soc Mech Eng 1996;118:36–43.
[81] Carcasci C, Costanzi F, Pacifici B. Performance analysis in off-design condition of gas turbine air-bottoming combined system. Energy Proc 2014;45:1037–46. https://doi.org/10.1016/j.egypro.2014.01.109.
[82] Nadir M, Ghenaiet A, Carcasci C. Thermo-economic optimization of heat recovery steam generator for a range of gas turbine exhaust temperatures. Appl Therm Eng 2016;106:811–26. https://doi.org/10.1016/j.applthermaleng.2016.06.035.
[83] Carcasci C, Pacifici B, Winchler L, Cosi L, Ferraro R. Thermoeconomic analysis of a one-pressure level heat recovery steam generator considering real steam turbine cost. Energy Proc 2015;82:591–8. https://doi.org/10.1016/j.egypro.2015.11.877.
[84] Carcasci C, Cosi L, Ferraro R, Pacifici B. Effect of a real steam turbine on thermoeconomic analysis of combined cycle power plants. Energy 2017;138:32–47. https://doi.org/10.1016/j.energy.2017.07.048.
[85] Toscotec introduces 100% hydrogen fuelled burners - tissue World Magazine. n.d, https://www.tissueworldmagazine.com/world-news/toscotec-introduces-100-hydrogen-fuelled-burners/. [Accessed 16 January 2023].
[86] Toscotec introduces 100% hydrogen fueled burners for sustainable papermaking: Toscotec. n.d. https://www.toscotec.com/en/news-article/toscotec-introduces-100-hydrogen-fueled-burners-for-sustainable-papermaking. [Accessed 16 January 2023].
[87] Zini M, Sodini R, Carcasci C. Modeling and optimization of a hospital gas turbine-based cogeneration system. https://doi.org/10.1115/1.4055418; 2022.
[88] Singlitico A, Østergaard J, Chatzivasileiadis S. Onshore, offshore or in-turbine electrolysis? Techno-economic overview of alternative integration designs for green hydrogen production into Offshore Wind Power Hubs. Renew Sustain Energy Transit 2021;1:100005. https://doi.org/10.1016/J.RSET.2021.100005.
[89] Lund H, Thellufsen JZ, Østergaard PA, Sorknæs P, Skov IR, Mathiesen BV. EnergyPLAN – advanced analysis of smart energy systems. Smart Energy 2021;1. https://doi.org/10.1016/J.SEGY.2021.100007.

[90] Bottecchia L, Lubello P, Zambelli P, Carcasci C, Kranzl L. The potential of simulating energy systems: the multi energy systems simulator model. Energies 2021;14:1–26. https://doi.org/10.3390/en14185724.
[91] Lubello P, Pasqui M, Mati A, Carcasci C. Assessment of hydrogen based long term electrical energy storage in residential energy systems. Smart Energy 2022;8: 100088. https://doi.org/10.1016/j.segy.2022.100088.
[92] Staffell I, Pfenninger S. Using bias-corrected reanalysis to simulate current and future wind power output. Energy 2016;114:1224–39. https://doi.org/10.1016/J.ENERGY.2016.08.068.
[93] Nikolaidis P, Poullikkas A. A comparative overview of hydrogen production processes. Renew Sustain Energy Rev 2017;67:597–611. https://doi.org/10.1016/J.RSER.2016.09.044.
[94] Ju HK, Badwal S, Giddey S. A comprehensive review of carbon and hydrocarbon assisted water electrolysis for hydrogen production. Appl Energy 2018;231: 502–33. https://doi.org/10.1016/J.APENERGY.2018.09.125.
[95] Schnuelle C, Wassermann T, Fuhrlaender D, Zondervan E. Dynamic hydrogen production from PV & wind direct electricity supply – Modeling and techno-economic assessment. Int J Hydrogen Energy 2020;45:29938–52. https://doi.org/10.1016/J.IJHYDENE.2020.08.044.
[96] Falcão DS, Pinto AMFR. A review on PEM electrolyzer modelling: guidelines for beginners. J Clean Prod 2020;261. https://doi.org/10.1016/J.JCLEPRO.2020.121184.
[97] Kharel S, Shabani B. Hydrogen as a long-term large-scale energy storage solution to support renewables. Energies 2018;11. https://doi.org/10.3390/en11102825.
[98] Superchi F, Mati A, Carcasci C, Bianchini A. Techno-economic analysis of wind-powered green hydrogen production to facilitate the decarbonization of hard-to-abate sectors: a case study on steelmaking. Appl Energy 2023;342:121198. https://doi.org/10.1016/j.apenergy.2023.121198.
[99] Puertollano green hydrogen plant - Iberdrola n.d. https://www.iberdrola.com/about-us/what-we-do/green-hydrogen/puertollano-green-hydrogen-plant (accessed July 7, 2023).
[100] Zini M, Cheli L, Carcasci C. Machine Learning-Based Energy Monitoring of Buildings: Development of a Systematic Method Applied to an Italian Case Study n.d. https://doi.org/10.2139/SSRN.4494892.
[101] Reis LRD, Camacho JR, Novacki DF. The Newton Raphson method in the extraction of parameters of PV modules, vol. 4; 2017. https://doi.org/10.24084/repqj15.416.
[102] Nicita A, Maggio G, Andaloro APF, Squadrito G. Green hydrogen as feedstock: financial analysis of a photovoltaic-powered electrolysis plant. Int J Hydrogen Energy 2020;45:11395–408. https://doi.org/10.1016/j.ijhydene.2020.02.062.
[103] Jang D, Kim K, Kim KH, Kang S. Techno-economic analysis and Monte Carlo simulation for green hydrogen production using offshore wind power plant. Energy Convers Manag 2022;263. https://doi.org/10.1016/J.ENCONMAN.2022.115695.
[104] Wang R, Lam C-M, Hsu S-C, Chen J-H. Life cycle assessment and energy payback time of a standalone hybrid renewable energy commercial microgrid: a case study of Town Island in Hong Kong. https://doi.org/10.1016/j.apenergy.2019.04.183; 2019.
[105] Kijo-Kleczkowska A, Bru'sbru's P, Więciorkowski G. Profitability analysis of a photovoltaic installation-A case study. Energy 2022;261:125310. https://doi.org/10.1016/j.energy.2022.125310.
[106] Yang Y, De La Torre B, Stewart K, Lair L, Phan NL, Das R, et al. The scheduling of alkaline water electrolysis for hydrogen production using hybrid energy sources. Energy Convers Manag 2022;257. https://doi.org/10.1016/J.ENCONMAN.2022.115408.
[107] Furfari S, Clerici A. Green hydrogen: the crucial performance of electrolysers fed by variable and intermittent renewable electricity. Eur Phys J Plus 2021;136. https://doi.org/10.1140/EPJP/S13360-021-01445-5.
[108] Fan JL, Yu P, Li K, Xu M, Zhang X. A levelized cost of hydrogen (LCOH) comparison of coal-to-hydrogen with CCS and water electrolysis powered by renewable energy in China. Energy 2022;242:123003. https://doi.org/10.1016/J.ENERGY.2021.123003.
[109] Haroon Bukhari M, Javed A, Ali Abbas Kazmi S, Ali M, Talib Chaudhary M. Techno-economic feasibility analysis of hydrogen production by PtG concept and feeding it into a combined cycle power plant leading to sector coupling in future. Energy Convers Manag 2023;282:116814. https://doi.org/10.1016/J.ENCONMAN.2023.116814.
[110] IRENA Renewable Cost Database. Renewable power generation costs in 2020. 2020.
[111] Gorre J, Ruoss F, Karjunen H, Schaffert J, Tynjälä T. Cost benefits of optimizing hydrogen storage and methanation capacities for Power-to-Gas plants in dynamic operation. Appl Energy 2020;257:113967. https://doi.org/10.1016/J.APENERGY.2019.113967.
[112] Adolfo D, Carcasci C, Pacifici B. A new correlation for estimating the gas turbine cost n.d. https://doi.org/10.1177/0957650921994388.
[113] The boiler room. n.d. http://www.boilerroom.com/budget.html. [Accessed 6 March 2023].
[114] Nicita A, Maggio G, Andaloro APF, Squadrito G. Green hydrogen as feedstock: financial analysis of a photovoltaic-powered electrolysis plant. Int J Hydrogen Energy 2020;45:11395–408. https://doi.org/10.1016/J.IJHYDENE.2020.02.062.
[115] Carbon price tracker | ember. n.d, https://ember-climate.org/data/data-tools/carbon-price-viewer/. [Accessed 6 March 2023].
[116] ARERA - Prezzi finali dell'energia elettrica per i consumatori industriali - Ue a Area euro n.d. https://www.arera.it/it/dati/eepcfr2.htm (accessed March 6, 2023).
[117] ARERA - Prezzi finali del gas naturale per i consumatori industriali - UE e area Euro n.d. https://www.arera.it/it/dati/gpcfr2.htm (accessed March 6, 2023).
[118] Zhao X, Fu L, Wang X, Sun T, Wang J, Zhang S. Flue gas recovery system for natural gas combined heat and power plant with distributed peak-shaving heat pumps. Appl Therm Eng 2017;111:599–607. https://doi.org/10.1016/J.APPLTHERMALENG.2016.09.130.
[119] Practical Considerations for Firing Hydrogen Versus Natural Gas – Combustion Engineering Association n.d. https://cea.org.uk/practical-considerations-for-firing-hydrogen-versus-natural-gas/(accessed February 24, 2023).
[120] Carbon intensity of electricity. n.d, https://ourworldindata.org/grapher/carbon-intensity-electricity. [Accessed 28 February 2023].
[121] Study on early business cases for H2 in energy storage and more broadly power to H2 applications. 2017.
[122] Mayer T, Semmel M, Alberto M, Morales G, Maria K, Bauer A, et al. Techno-economic evaluation of hydrogen refueling stations with liquid or gaseous stored hydrogen. Int J Hydrogen Energy 2019;44:25809–33. https://doi.org/10.1016/j.ijhydene.2019.08.051.
[123] Moran C, Moylan E, Reardon J, Gunawan TA, Deane P, Yousefian S, et al. A flexible techno-economic analysis tool for regional hydrogen hubs – a case study for Ireland. Int J Hydrogen Energy 2023. https://doi.org/10.1016/J.IJHYDENE.2023.04.100.
[124] H2 in the underground: are salt caverns the future of hydrogen storage? | ENGIE Innovation. n.d. https://innovation.engie.com/en/articles/detail/hydrogen-underground-storage-salt-caverns/25906/general. [Accessed 12 July 2023].
[125] International Energy Agency I. Global hydrogen review 2022. 2022.
[126] IRENA. World energy transitions outlook. Irena 2022:1–54.
[127] EU natural gas - 2023 data - 2010-2022 historical - 2024 forecast - price - quote. n.d, https://tradingeconomics.com/commodity/eu-natural-gas. [Accessed 3 March 2023].